

0
(DOI: will be inserted by hand later)
© ESO 2006

The exotic chemical composition of the Sagittarius dwarf Spheroidal galaxy

L. Sbordone^{1,2,4}, P. Bonifacio^{1,2,3}, R. Buonanno^{5,8}, G. Marconi⁶, L. Monaco⁶, and S. Zaggia⁷

¹ CIFIST Marie Curie Excellence Team

² Observatoire de Paris, GEPI, 5, place Jules Janssen, 92195 Meudon, France

e-mail: luca.sbordone@obspm.fr

³ INAF – Osservatorio Astronomico di Trieste – via G. B. Tiepolo 11, 34131 Trieste, Italy

⁴ INAF – Osservatorio Astronomico di Roma – via di Frascati 33, 00040 Monte Porzio Catone, Rome, Italy

⁵ Università di Roma “Tor Vergata”, via della Ricerca Scientifica 1, 00133 Rome, Italy

⁶ ESO – European Southern Observatory, Alonso de Cordova 3107, Santiago, Chile

⁷ INAF – Osservatorio Astronomico di Padova, Vicolo dell’Osservatorio 5, 35122 Padua, Italy

⁸ ASI Science Data Center, via Galileo Galilei, 00044 Frascati, Italy

ABSTRACT

Context. The Sagittarius dwarf Spheroidal Galaxy is the nearest neighbor of the Milky Way. Moving along a short period quasi-polar orbit within the Halo, it is being destroyed by the tidal interaction with our Galaxy, losing its stellar content along a huge stellar stream.

Aims. We study the detailed chemical composition of 12 giant stars in the Sagittarius dwarf Spheroidal main body, together with 5 more in the associated globular cluster Terzan 7 by means of high resolution VLT-UVES spectra.

Methods. Abundances are derived for up to 21 elements from O to Nd, by fitting lines EW or line profiles against ATLAS 9 model atmospheres and SYNTHE spectral syntheses calculated ad-hoc. Temperatures are derived from $(V-I)_0$ or $(B-V)_0$ colors, gravities from Fe I - Fe II ionization equilibrium.

Results. The metallicity of the observed stars is between $[Fe/H]=-0.9$ and 0. We detected a highly peculiar “chemical signature”, with undersolar α elements, Na, Al, Sc, V, Co, Ni, Cu and Zn among others, and overabundant La, Ce and Nd. Many of these abundance ratios (in particular light-odd elements and iron peak ones) are strongly at odds with what is observed within the Milky Way, they thus may be a very useful tool to recognize populations originated within the Sagittarius dwarf. This can be clearly seen in the case of the globular Palomar 12, which is believed to have been stripped from Sagittarius: the cluster shows precisely the same chemical “oddities”, thus finally confirming its extragalactic origin.

Key words. Stars: abundances – Stars: atmospheres – Galaxies: abundances – Galaxies: dwarf – Galaxies: individual: Sgr dSph – Globular Clusters: individual: Terzan 7

1. Introduction

Dwarf Spheroidal Galaxies (dSph) have become in recent years a highly popular subject of investigation. The interest towards such objects has been largely driven by the key role they are supposed to play in the buildup process of larger galaxies such as the Milky Way. The available detailed abundance ratios for stars in Local Group (LG) dSph are nevertheless showing that *present day* dSph are undesirable candidates as hierarchical merging building blocks (see Vladilo et al., 2003; Venn et al., 2004, and references therein). The distinctive abun-

dance ratios (most notably, the low $[\alpha/Fe]$ ratio) observed in the LG dSph hint for star formation histories remarkably different from the one characteristic of the MW, thus making it difficult, for *evolved* dSphs to have played a significant role in building up our Galaxy. Such findings are, after all, not surprising: undisturbed, low mass dSph are a different environment from the MW, where low star formation rates and highly efficient galactic winds have likely played a major role (Lanfranchi & Matteucci, 2003, 2004; Lanfranchi et al., 2006). Dwarf Spheroidals are nevertheless not ruled out as MW “building blocks”, but the main merging phase should have taken place at

Send offprint requests to: L. Sbordone

arXiv:astro-ph/0612125 v1 5 Dec 2006

a very early stage, allowing the subsequent evolution to differentiate the surviving dSph from the larger, merged structures.

Nevertheless, at least one major merging episode is currently taking place in the MW, at expenses of the Sagittarius dSph (Sgr dSph, Ibata, Gilmore, & Irwin, 1994, 1995). The nearest known dSph (26.3 Kpc, Monaco, Bellazzini, Ferraro, & Pancino, 2004), Sgr dSph is being tidally destroyed while moving along its quasi-polar, short period (less than 1 Gyr) orbit around the MW (Ibata et al., 1997; Helmi & White, 1999), and its stars are dispersing along a huge stream in the Halo (Majewski, Skrutskie, Weinberg, & Ostheimer, 2003; Belokurov et al., 2006).

In previous works (Bonifacio et al., 2000, 2004; Sbordone et al., 2005, henceforth paper I, II and III respectively) we presented chemical abundance for total 12 stars in the Sgr dSph main body and in the associated globular cluster Terzan 7. Paper I reported abundances for 20 elements from O to Eu in two Sgr dSph main body stars, paper II added Fe and α elements for 10 more stars, while paper III analyzed Fe, α elements and Ni in 5 giants in Terzan 7. In two more papers, we have also obtained iron and α elements abundances for 15 brighter RGB stars of Sgr (Monaco et al., 2005), and Sulphur abundances for three stars in Ter 7 (Caffau, Bonifacio, Faraggiana, & Sbordone, 2005). The present paper unifies, extends and revisits the results presented in Paper I, II and III:

- the temperature scale has been recalibrated for the 12 Sgr dSph main body stars, by using photometries and reddening from Monaco, Ferraro, Bellazzini, & Pancino (2002). This has been made to homogenize the temperature scale with the one used in Monaco et al. (2005). See section 2 for details;
- the array of abundances has been extended to up to 21 species including O, Na, Mg, Al, Si, Ca, Sc, Ti, V, Cr, Mn, Fe, Co, Ni, Cu, Zn, Y, Ba, La, Ce, and Nd;
- with respect to the previous papers, updated atomic data are used for Mg, Ca, La, Ce, and Nd.

2. Observations, data reduction and analysis

As above stated, the present work uses the same data employed in Paper I and II for the Sgr dSph main body, and in Paper III for Terzan 7 stars. The reader is thus referred there for the details of the observations. Table 1 lists photometry and derived atmospheric parameters for the 12 Sgr dSph main body and the 5 Ter 7 giants, a sample of the spectra for the 12 Sgr dSph stars is shown in fig. 1 of Paper II, and in fig. 1 of Paper III for the 5 Ter 7 giants. The temperature scale was recalibrated in Sgr dSph main body due to the adoption of Monaco, Ferraro, Bellazzini, & Pancino (2002) photometry and Layden & Sarajedini (2000) reddening, while in Paper I and II we used Marconi et al. (1998) photometry and reddening estimates. This change came from the need of using a temperature scale homogeneous across our present work, and applicable to future

studies also. Moreover Monaco, Ferraro, Bellazzini, & Pancino (2002) photometry covers a much larger field and it was used as a basis for FLAMES candidates selection (see Zaggia et al., 2004).

Effective temperatures were derived from dereddened (V-I) colors by means of the Alonso, Arribas, & Martínez-Roger (1999, 2001) calibration for giant stars. The change in the photometry and reddening correction ($E(V-I)=0.22$ in Marconi et al. 1998 were substituted by $E(V-I)=0.18$ from Layden & Sarajedini 2000¹. led to significantly *lower* derived effective temperatures, with a mean decrease of about 250 K. The reason for such a change comes partly from the different reddening estimates (0.04 difference in V-I color), but is mainly due to an offset between the two photometries (0.074 mean). **As a further test, we checked the temperatures derived from 2MASS J-K colors for stars in this work and in Monaco et al. (2005). Nevertheless, the Sgr dSph stars presented here are generally too faint for 2MASS to provide reliable colors for them, and the derived temperatures were scattered over more than 1000 K. For the Monaco et al. (2005) stars, 2MASS J-K colors led to temperatures in average 75 K hotter than the ones based on Monaco, Ferraro, Bellazzini, & Pancino (2002) V-I colors, while on Ter 7 there was no systematic discrepancy between the two temperature scales.** We will show further on (see 3.3) how the changes in the physical parameters of the atmospheres do not alter significantly the “scientific output” of this research.

Similarly to what we did in paper I through III, one-dimensional, LTE atmosphere models were computed for the observed stars by means of our GNU-Linux ported version of the ATLAS code. ATLAS 9 (using Opacity Distribution Functions, henceforth ODF) models were used for all the stars except for star #1665 in Terzan 7 which required an ATLAS 12 (opacity sampling) model due to its very low temperature and gravity (see Sbordone et al., 2005, for details). For the ODF based models, no α -enhancement was assumed (since $[\alpha/Fe]$ appears to be solar or sub-solar); “new” type ODF (Castelli & Kurucz, 2003) were used. Abundances were computed from measured line equivalent widths (EW) by means of WIDTH, model gravity was set by imposing Fe I – Fe II ionization equilibrium, and microturbulence by requesting abundances of Fe I lines to be independent of the line EW. Abundances for lines affected by strong hyperfine splitting, or for which EW measurement was problematic (e. g. the 630 nm OI line) were derived by spectral synthesis, using SYNTH (for ATLAS, WIDTH and SYNTH see Kurucz, 1993, 2005; Sbordone, Bonifacio, Castelli, & Kurucz, 2004; Sbordone, 2005B).

To produce the same Fe II line strength with a lower T_{eff} , lower gravity is needed. Our gravity estimates decreased by about 0.3 – 0.4 dex with respect to the ones in paper II, leading

¹ Reddening estimate from Schlegel et al. (1998) is very near to the Layden & Sarajedini (2000) one, with typical value of $E(V-I)=0.19$ for our Sgr dSph main body stars

Table 1. Photometry and atmospheric parameters for the studied stars. Employed colors are (V-I)₀ for Sgr dSph main body and (B-V)₀ for Ter 7. Coordinates can be found in Paper II (Sgr dSph main body) and Paper III (Ter 7).

Star	V mag	(V-I) ₀ mag	T _{eff} K	log g cgs	ξ kms ⁻¹
Sgr 432	17.700	1.013	4713	2.2	1.20
Sgr 628	18.228	1.040	4656	2.1	1.75
Sgr 635	18.186	1.074	4588	2.1	1.50
Sgr 656	18.217	1.008	4723	2.1	1.50
Sgr 709	18.260	1.034	4669	2.2	1.20
Sgr 716	18.282	1.012	4715	2.1	1.60
Sgr 717	18.282	1.007	4726	2.0	1.10
Sgr 772	18.392	1.070	4596	1.9	1.60
Sgr 867	18.465	1.031	4675	1.7	1.95
Sgr 879	18.516	1.073	4590	1.9	1.30
Sgr 894	18.507	1.067	4602	2.1	1.50
Sgr 927	18.580	1.079	4578	2.1	1.30
(B-V)₀					
Ter7 1272	16.62	1.15	4421	1.2	1.45
Ter7 1282	16.08	1.30	4203	1.3	1.60
Ter7 1515	16.76	1.12	4468	2.0	1.45
Ter7 1665	15.04	1.50	3945	0.8	1.60
Ter7 1708	16.08	1.28	4231	1.2	1.70

to values of $\log g \sim 2.1$. This caused the compatibility between isochrone and ionization gravities to worsen somewhat in comparison with Paper I and II: superimposing Girardi et al. (2002) isochrones of compatible age and metallicity leads now to derive typical gravities of the order of $\log g \sim 2.4$, for a mean discrepancy of about 0.35 dex.

Complete line lists, with employed $\log gf$ values, measured EW and derived abundances are available in the online version. An excerpt is available in table 2. Paper I and II employed the same set of lines and atomic data (with the exception of O I 630 nm line) for the elements which were common among the two. Paper III used the same set of lines of Paper I and II for the Dichroic I spectra and (obviously) a different one for the Dichroic II spectra. Nevertheless, in Paper III $\log gf$ were updated for Mg and Ca lines. Globally, updates are as follows:

- **O I** we used the Storey & Zeippen (2000) $\log gf$ already from Paper II on. O I 630 nm line is measured by spectral synthesis. The line is heavily blended with a weak Ni I feature for which we used the Johansson et al. (2003) laboratory $\log gf$;
- **Mg I** from Paper III on, where applicable we use the Gratton et al. (2003) $\log gf$;
- **Si I** solar Edvardsson et al. (1993) $\log gf$ values are used where applicable;

- **Ca I** since Paper III we use, where present, Smith & Raggett (1981) furnace $\log gf$; 586.7 nm line has Gratton et al. (2003) $\log gf$;
- **Zn I** we used the $\log gf$ values of Biemont & Godefroid (1980) which provide a good agreement between the photospheric and the meteoritic Zn abundance;
- **La II** recent $\log gf$ values from Lawler et al. (2001) are used here when available;
- **Ce II** $\log gf$ values are taken from Hill et al. (1995);
- **Nd II** new $\log gf$ values are taken from Den Hartog et al. (2003);

All the other atomic data are the ones provided in the line lists included with our ATLAS suite port ², which come from R. L. Kurucz website ³. Hyperfine splitting was used to synthesize lines for Mn I, Co I, Cu I. Solar isotopic ratios were assumed.

Many of the employed Na and Al lines are known to be significantly affected by NLTE (Baumüller & Gehren, 1997; Baumüller et al., 1998; Gratton et al., 1999). NLTE corrections are generally a function of metallicity, atmospheric parameters and line strength, and unfortunately no correction computations have been produced for Al lines for giant stars such the one we are dealing with. As a consequence, we publish LTE abundances for Al. For Na lines, correction are computed for giant stars by Gratton et al. (1999). Their grid extends down to $\log(g)=1.5$ and $T_{eff}=4000$ K, which fits all the Sgr dSph main body stars and one of the Ter 7 stars. For these stars we interpolated the correction values and present here the corrected abundances. The other four Ter 7 stars go beyond the grid in gravity or temperature, or both. In these cases, extrapolated values can be used, but given the complex behavior of NLTE corrections in phase space, we preferred to adopt a single value of $A_{NLTE}-A_{LTE}=0.2$.

3. Results

Absolute abundances for Sgr dSph stars, solar assumed abundances, [Fe/H], [X/Fe] and associated errors are listed in table 4 and 5. The same data for Terzan 7 stars are in table 6.

3.1. The Sgr dSph main body

As already stated in Paper I and II, the 12 Sgr dSph stars have a relatively high mean metallicity ([Fe/H] between -0.89 and 0.02): the average value is [Fe/H]=-0.36. In comparison with Paper I and II, the variation in the atmospheric parameters led to a slight metallicity decrease.

A full picture of the “chemical signature” of Sgr dSph main body is presented in figure 2. At first glance, Sgr dSph appears to bear the signs of a highly peculiar chemical evolution. We will now treat in some detail the various element groups.

² Available at <http://wwwuser.oat.ts.astro.it/atmos/>

³ <http://kurucz.harvard.edu/>

Table 2. An excerpt from the detailed line tables available in the Online version. Employed lines, $\log gf$ values, $\log gf$ sources, observed EW and derived abundances for Sgr dSph stars # 432 to #716. Codes for the source of the $\log gf$ can be found in the bibliography. For lines that have been synthesized, “syn” substitutes the EW. LTE abundances are listed here for the Na lines.

Ion	λ (nm)	$\log gf$	source of $\log gf$	EW (pm) 432	A(X)	EW (pm) 628	A(X)	EW (pm) 635	A(X)	EW (pm) 656	A(X)	EW (pm) 709	A(X)	EW (pm) 716	A(X)
O I	630.0304	-9.717	STZ	syn	8.03	syn	8.35	syn	8.33	syn	8.15	syn	8.50	syn	8.54
Na I	568.2633	-0.700	KP	—	—	10.67	5.79	7.56	5.33	9.61	5.76	11.23	6.06	11.18	5.94
Na I	615.4227	-1.560	KP	—	—	4.38	5.72	1.95	5.21	3.36	5.62	—	—	2.47	5.44
Na I	616.0747	-1.260	KP	—	—	5.26	5.56	3.60	5.26	4.34	5.49	6.07	5.74	5.77	5.69

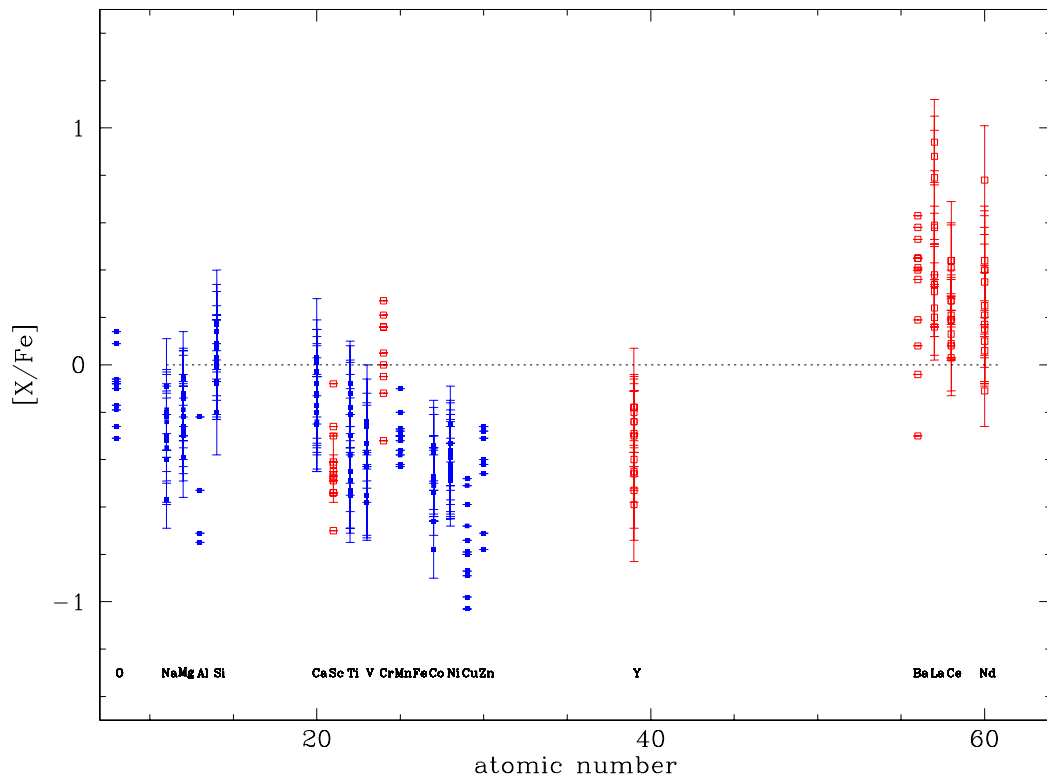


Fig. 2. The “chemical signature” of the 12 Sgr dSph stars: $[X/Fe]$ ratios are plotted against atomic number. The dashed line at 0 value represents the solar abundance ratios. As in tab. 4, 5 and 6, ratios are against Fe I for neutral species (filled squares), against Fe II for the ionized ones (Sc, Cr, Y, Ba, La, Ce, Nd, open squares). Error bars are the same listed in tab. 4, 5 and 6, so that species measured on a single line do not show any error bar. Important departures from solar ratios can be seen throughout all the sampled elements: see text for details.

The α elements show the same behavior already described in Paper I and II (fig. 3). The α elements show solar or undersolar ratio against iron, with a significant trend with the metallicity, leading in particular Mg and Ca to reach heavy underabundances in the most metal rich stars of the sample. ($[Mg/Fe] = -0.39$ in star #709). Silicon remains instead nearer to solar values, and even shows some enhancement in some cases ($[Si/Fe] = 0.18$ in star #894). Titanium, (although its inclusion

among α elements is not totally correct from a nucleosynthetic point of view, see Burbidge et al., 1957) also shows heavy underabundance compared to solar values.

Light odd-atomic number elements Na, Al, Sc and V also show a highly significant underabundance with respect to solar values (see fig. 1). A hint of a trend with metallicity can be seen in $[Al/Fe]$ graph, but since in Sgr dSph main body stars a single

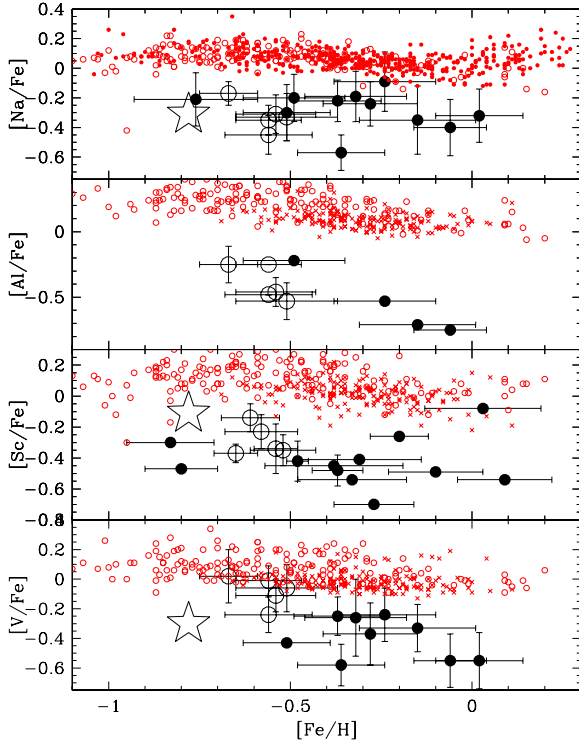


Fig. 1. [Na/Fe], [Al/Fe], [Sc/Fe] and [V/Fe] plotted against [Fe/H]. The symbols are as follows: large filled circles, Sgr dSph main body, large open circles Ter 7, large star, Palomar 12 (mean value for the stars in Cohen, 2004), small open circles, MW sample from Reddy et al. (2006) small crosses, MW sample from Reddy et al. (2003), small filled circles, MW sample from Venn et al. (2004), which also includes Reddy et al. (2003) stars. In the Na plot, the value for Pal 12 has been corrected by the same amount used for low-gravity Ter 7 stars ($A_{NLTE} - A_{LTE} = 0.2$)

line was used, and considering the possible presence of NLTE effects, this cannot be considered significant.

Iron-peak elements Co, Ni, Cu and Zn (fig. 4) display perhaps the most intriguing anomalies, showing constantly undersolar ratios, with no clear metallicity trends. Although both Cu and Zn have been measured using a single line, these are rather strong and clear transitions whose fit is robust.

Finally, heavy n-capture elements Y, Ba, La, Ce and Nd (Y, Ba, La and Nd in fig. 5) also show interesting patterns. Y appears to be undersolar at low metallicity, with a slight increasing trend with metallicity which leads to solar [Y/Fe] ratios around solar [Fe/H]. Ba is oversolar with a moderate increasing trend with metallicity, and generally outside the range of [Ba/Fe] variation within the MW, but three Sgr dSph main body stars (#635, #716 and #867) show MW-like [Ba/Fe] ratios. Spectra inspection did not show clear anomalies in the Ba lines in these stars, but, since we are using a single Ba II feature, the hypothesis of some contamination of the line cannot

be ruled out. Lanthanum abundances show an above than average spread, but [La/Fe] appears to be consistently oversolar and increasing with metallicity, reaching rather extreme values at solar metallicity ([La/Fe]=0.94 at [Fe/H]=0.02 in star #709). Finally, Nd starts from MW-like (essentially solar) ratios at low metallicity, increasing then slightly but never truly standing out with respect to the values observed within the MW.

3.2. Terzan 7

In figures 3 through 5 Ter 7 stars are always represented by large open circles. As can be seen, Ter 7 chemical composition appears to closely match the one observed in the Sgr dSph main body at corresponding metallicity. Nevertheless some differences can be seen: ratios against iron are slightly above the Sgr dSph values for V, Co, Ni, Y and Nd. This can be probably due to the lower reliability of the analysis in such low gravity – low temperature atmospheres.

3.3. Error budget

In table 3 we report the variations in abundances, [X/Fe] and [Fe/H] for star # 656, as due to the variation in atmospheric parameters between Paper I / II and this work. This allows to estimate the impact of systematic uncertainties in the model parameters. Star # 656 was the one with the largest temperature variation in the sample ($\Delta T_{eff} = -396K$, $\Delta \log g = -0.4$, $\Delta \xi = -0.15 \text{ km s}^{-1}$, new - old). Despite such a large variation in the parameters, [X/Fe] values show remarkably low changes.

3.4. Comparison with other results

The only high resolution abundance analysis in the Sgr dSph independent of those of our group, is the one presented in McWilliam et al. (2003,B); McWilliam & Smecker-Hane (2005,B). The authors analyze a sample of 14 Sgr dSph main body giants, with higher luminosity and lower temperatures than the ones presented in this work. The bulk of their sample lies in the same metallicity range we explore here, while three stars lie below [Fe/H]=-1. Despite the difference in stellar parameters and in the details of the performed analysis, the results are largely coincident: Al, Na and Cu undersolar ratios are detected, aside with a positive [La/Fe], with increasing trend with the metallicity. The authors derive slightly higher [α /Fe] ratios than we do, but not by a significant amount. The undersolar [Mn/Fe] ratio detected in McWilliam et al. (2003,B) is also confirmed by our results, but the lack in our sample of stars below [Fe/H]=-1 does not allow us to confirm also the presence of an increasing trend of [Mn/Fe] with metallicity. In McWilliam & Smecker-Hane (2005) the bulk of the analyzed stars show [Cu/Fe]~ -0.5, coincident with what we find. This is interesting since a different Cu I feature is sampled with respect to the one we use. However four stars show significantly higher Cu content ([Cu/Fe]~0.3), something we do not detect.

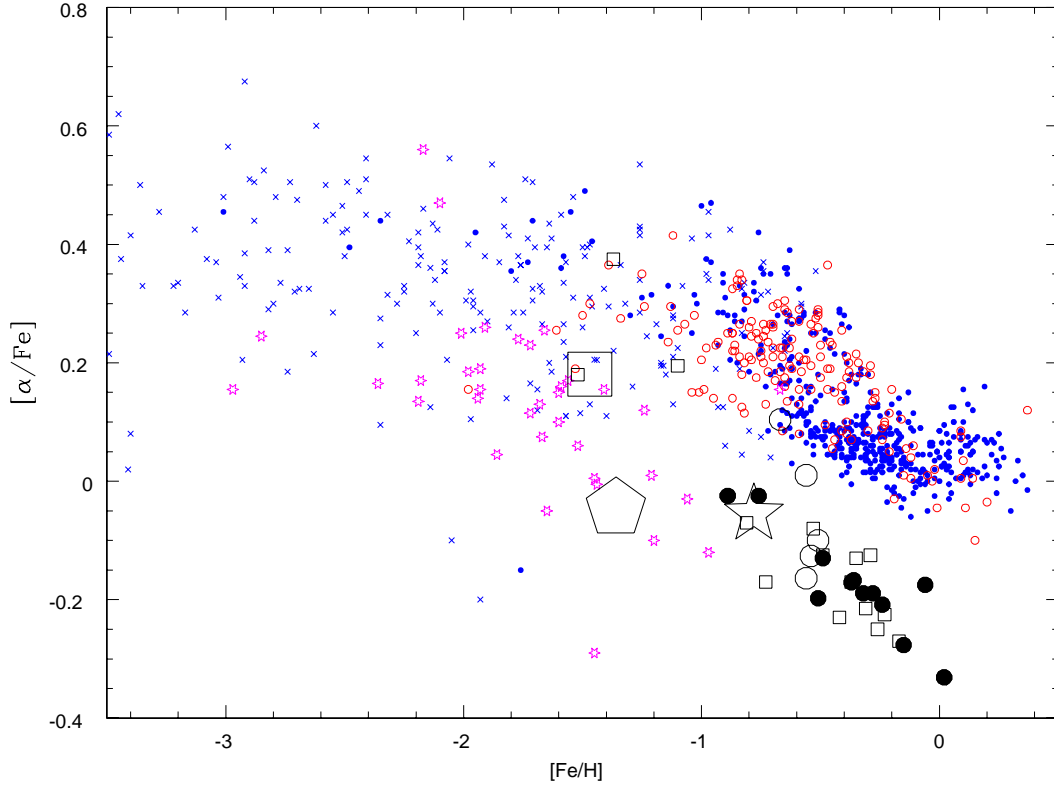


Fig. 3. $[\alpha/\text{Fe}]$ (defined as mean of $[\text{Mg}/\text{Fe}]$ and $[\text{Ca}/\text{Fe}]$) is plotted against $[\text{Fe}/\text{H}]$ for various samples: large filled dots, Sgr dSph main body (this work); large open dots, Ter 7 (this work); open squares, Sgr dSph main body upper RGB stars (Monaco et al., 2005), small open stars, LG dSph stars (Car, Dra, For, Leo I, Scl, Sex, UMi, Shetrone et al., 2001, 2003). Small symbols refer to MW samples: filled circles, Venn et al. (2004) thin and thick disk stars; crosses, Venn et al. (2004) Halo stars; open circles, Reddy et al. (2006), mainly thick disk stars. Huge open symbols refer to mean values for globular clusters: star, Palomar 12 (4 stars, Cohen, 2004); square M 54 (5 stars, Brown et al., 1999); pentagon, Ruprecht 106 (2 stars, Brown et al., 1997). Ru 106 is included due to its low $[\alpha/\text{Fe}]$, $[\text{Ni}/\text{Fe}]$ ratios and its high radial velocity, hinting for an extragalactic origin, although its association with Sgr dSph is unlikely (see Pritzl et al., 2005).

The composition of three of our 5 Ter 7 giants (# 1282, #1665 and # 1708) has been studied by Tautvaišienė et al. (2004). We already compared our results with the ones of Tautvaišienė et al. (2004) in Paper III regarding atmosphere parameters, Iron and α element abundances. Regarding the other elements, while many the overall trends match (undersolar Na and Al, oversolar La...), some are at odd with our results (Sc, V, Mn, Co, Cu among others). As already stated in Paper III, the atmosphere parameters are fully consistent among us and Tautvaišienė et al. (2004), thus these discrepancies should be due to differences in the line data employed. Nevertheless, the fact that Tautvaišienė et al. (2004) perform a differential analysis makes the comparison quite difficult.

3.5. The long lost Pal 12

In figures 3 through 5, the average value of Palomar 12 stars abundances from Cohen (2004) are shown as large open star symbols. By comparing these results against the limited sample

of Sgr dSph abundances available at that time, Cohen (2004) already deduced that the strong similarities between the two objects pointed towards a formation of Palomar 12 within the Sgr dSph system. With the present work, the resemblance between Pal 12 and Sgr dSph appears even more clearly: Pal 12 displays precisely the same “chemical signature” encountered within Sgr dSph even in its most pronounced anomalies, such as the strong Na, Al, Co, Ni Cu and Zn underabundances. This leads to two main results: first, *the origin of Pal 12 within the Sgr dSph can be considered as finally established*. There is no known trace of chemically similar populations inside the MW. It can be hypothesized that another (now destroyed) dwarf galaxy may have dropped Pal 12 within the Halo, but such object should have been a sort of “twin” of Sgr dSph from an evolutive point of view. The proximity of Pal 12 to the Sgr dSph stream in parameter space is also well known. The second, possibly more intriguing result, is that *looking for a Sgr-like “signature” in the chemistry of a stellar population is a very effective tool to search for Sgr dSph debris within the MW*, at least

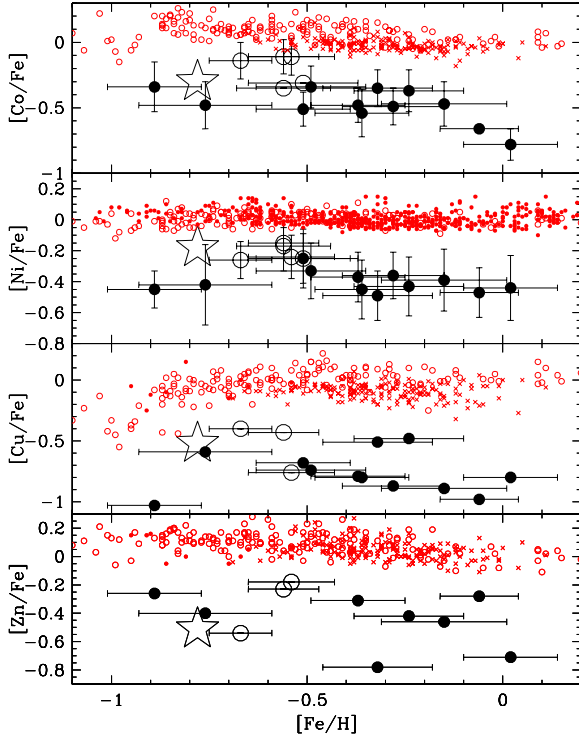


Fig. 4. $[\text{Co}/\text{Fe}]$, $[\text{Ni}/\text{Fe}]$, $[\text{Cu}/\text{Fe}]$ and $[\text{Zn}/\text{Fe}]$ plotted against $[\text{Fe}/\text{H}]$. The symbols are the same as in fig. 1, except for small filled circles, which indicate Venn et al. (2004) sample for Ni, and Bihain et al. (2004) sample for Cu and Zn.

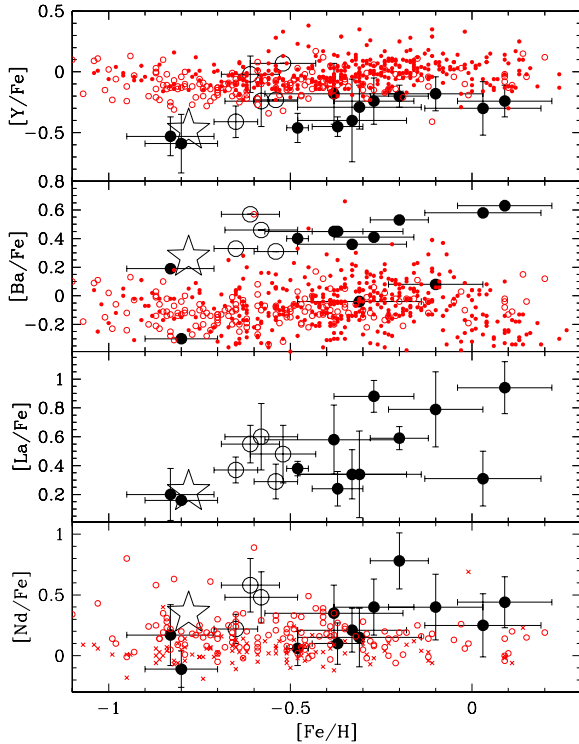


Fig. 5. $[\text{Y}/\text{Fe}]$, $[\text{Ba}/\text{Fe}]$, $[\text{La}/\text{Fe}]$ and $[\text{Nd}/\text{Fe}]$ plotted against $[\text{Fe}/\text{H}]$. Same symbols as in fig. 1

Table 3. Variations in the derived abundances $[\text{X}/\text{Fe}]$ and $[\text{Fe}/\text{H}]$ for star # 656 due to the change in atmospheric parameters between this work and Paper I, II. Absolute abundances from Paper II and this work are also listed to ease the comparison. Na abundances are listed here *without* the NLTE correction used elsewhere.

ion	A(X) Paper I / II	A(X) this work	$\Delta A(\text{X})$ new - old	$\Delta[\text{X}/\text{Fe}]$ new - old
O I	8.50	8.15	-0.35	-0.15
Na I	5.80	5.62	-0.18	0.02
Mg I	7.10	6.99	-0.11	0.09
Al I	—	—	—	—
Si I	7.31	7.25	-0.06	0.14
Ca I	6.09	5.96	-0.13	0.07
Sc II	2.55	2.34	-0.21	0.06
Ti I	4.78	4.44	-0.34	-0.14
V I	3.80	3.38	-0.42	-0.22
Cr II	5.55	5.45	-0.10	0.17
Mn I	5.08	4.75	-0.33	-0.13
Fe I	7.33	7.13	-0.20	—
Fe II	7.39	7.12	-0.27	-0.07
Co I	4.59	4.07	-0.52	-0.32
Ni I	5.77	5.51	-0.26	-0.06
Cu I	3.44	3.05	-0.39	-0.19
Zn I	3.94	3.92	-0.02	0.17
Y II	1.93	1.68	-0.25	0.02
Ba II	2.28	2.20	-0.08	0.18
La II	1.63	1.33	-0.30	-0.03
Ce II	1.65	1.29	-0.36	-0.09
Nd II	1.86	1.47	-0.39	-0.12

at not too low metallicity. Many of the Sgr dSph chemical oddities appear at any metallicity within the explored range, but it cannot be safely inferred what would happen of them at, say, $[\text{Fe}/\text{H}] = -2$. The α elements trend seems to resemble the one in MW populations below $[\text{Fe}/\text{H}] = -1$ (see fig. 3), while $[\text{Cu}/\text{Fe}]$ is known to drop in the MW below $[\text{Fe}/\text{H}] = -1$. Further analysis of low-metallicity Sgr dSph stars is needed to clarify this.

4. Discussion and Conclusions

From the observational point of view, our results can be summarized as follows:

1. The chemical composition of Sgr dSph main population is significantly at odds with respect to the one observed within the MW. Many elements (Na, Al, Sc, α elements, Co, Ni, Cu, Zn...) show significant underabundances when compared to MW stars of similar iron content. Such chemical

oddities are exactly replicated within the associated globular cluster Terzan 7.

2. Even more interesting, precisely the same “chemical signature” is displayed by Palomar 12. This, as already noted by Cohen (2004) essentially proves that this globular cluster originated within the Sgr dSph system to be subsequently stripped by the MW.

From the phenomenological point of view, this has one main consequence: chemical composition should allow to distinguish also *other* stellar populations which were stripped from Sgr dSph and added to the MW, at least for metallicities above $[\text{Fe}/\text{H}]=-1$. For lower metallicities, the survival of many of the chemical “markers” should be confirmed, but may be inferred in many cases by the absence of metallicity trends within them (e. g. Na, Ni, Zn).

It has nevertheless to be taken into account the absence, in the known MW populations, of stars of Sgr-like characteristics. Recently Chou et al. (2006) claimed the detection of metallicity gradients within the Sgr dSph stream, in the sense of higher metallicities in the populations stripped more recently from the galaxy. From this finding, we can infer that a significant chemical evolution took place in the galaxy since the most distant stream stars were stripped, or (more likely) that the outermost parts of Sgr dSph (the first to be stripped) were significantly more metal poor than the nucleus. A combination of both scenarios is also possible. In all these cases, the “chemical signature” we detect in the main body of Sgr dSph may well be much weaker, or undetectable in the Halo at metallicities below $[\text{Fe}/\text{H}]=-1$. Conversely, Palomar 12 stands as an unmistakable example of how evident this signature can be in more chemically evolved stars.

It appears a much harder task to decrypt the meaning of these abundances in terms of the chemical history of Sgr dSph, and we will not attempt to go deep in this regard in the present paper. Sgr dSph appears to have experienced a very long star formation and chemical evolution history. The lowest metallicity observed within the galaxy is about $[\text{Fe}/\text{H}]=-3$ (Zaggia et al., 2004), while the associated globulars (M 54, Ter 7, Ter 8, Arp 2, Pal 12) are dispersed between $[\text{Fe}/\text{H}]=-2$ and $[\text{Fe}/\text{H}]=-0.6$. At least the last few GYr of the galaxy evolution have taken place within the strong MW tidal field, which should have heavily influenced both its star formation and its yields retention capability. This may help explaining both the high mean metallicity of Sgr dSph and its scarce gas content in spite of having formed stars until a relatively recent past (likely a couple of GYr, see Paper II). At the same time, this may call for past (pre-interaction) Sgr dSph as being a relatively large, star forming, gas-rich object with a nucleated structure (Monaco et al., 2005B) and a rich set of globular clusters.

The detailed abundance ratios we present need to be interpreted in the framework of a detailed chemical evolution model taking into account galactic winds (such as in Lanfranchi & Matteucci, 2003, 2004; Lanfranchi et al., 2006; Lanfranchi, Matteucci & Cescutti, 2006B). Galactic winds appear to play a

key role in the evolution of small systems such as dSph, where they develop thanks to the relatively weak gravitational field these small galaxies create. Nevertheless, they still are more inferred than modeled, due to the great difficulty of the hydrodynamical calculations that would be needed. In the particular case of Sgr dSph, the influence of the MW tidal field likely favored the wind formation, an effect that has been most likely *time dependent*, since Sgr dSph orbit should have degraded with time.

Aside from the quoted issues, we want to stress how the presented abundances should not be taken as plainly representative of Sgr dSph “as a whole”. This not only comes from the small range in metallicity covered, but also from the small angular area from which they have been collected. Chou et al. (2006) findings point towards a scenario in which pre-interaction Sgr dSph may have showed strong metallicity gradients, or maybe even an incomplete chemical mixing. Especially at low metallicities, chemical enrichment may have been locally influenced by a small number of SN II, due to the low total mass of the galaxy. Larger sampling across the galaxy body and the streams are needed, as well as analyses of the more metal poor components, to be able to trace the full story of this fascinating neighbor.

Acknowledgements. LS, PB and SZ acknowledge support from the MIUR/PRIN 2004025729_002; LS and PB are supported also by EU contract MEXT-CT-2004-014265 (CIFIST). This work has made use of NASA’s Astrophysics Data System Bibliographical Services and of NIST online database of atomic data.

References

- Alonso, A., Arribas, S., & Martínez-Roger, C. 2001, *A&A*, 376, 1039
- Alonso, A., Arribas, S., & Martínez-Roger, C. 1999, *A&AS*, 140, 261
- Arnesen, A., Bengtsson, A., Hallin, R., Lindskog, J., Nordling, C., & Noreland, T. 1977, *Phys. Scripta* 16, 31 (log gf: ABH)
- Baumüller, D., Butler, K., & Gehren, T. 1998, *A&A*, 338, 637
- Baumüller, D., & Gehren, T. 1997, *A&A*, 325, 1088
- Belokurov, V., et al. 2006, *ApJ*, 642, L137
- Bielski, A. 1975, *JQSRT* 15, 463 (log gf: BIEL)
- Biemont, E., & Godefroid, M. 1980, *A&A*, 84, 361 (log gf: BG)
- Bihain, G., Israelian, G., Rebolo, R., Bonifacio, P., & Molaro, P. 2004, *A&A*, 423, 777
- Bonifacio, P., Sbordone, L., Marconi, G., Pasquini, L., & Hill, V. 2004, *A&A*, 414, 503
- Bonifacio, P., Hill, V., Molaro, P., Pasquini, L., Di Marcantonio, P., & Santin, P. 2000, *A&A*, 359, 663
- Brown, J. A., Wallerstein, G., & Gonzalez, G. 1999, *AJ*, 118, 1245
- Brown, J. A., Wallerstein, G., & Zucker, D. 1997, *AJ*, 114, 180

- Burbidge, E. M., Burbidge, G. R., Fowler, W. A., & Hoyle, F. 1957, *Reviews of Modern Physics*, 29, 547
- Caffau, E., Bonifacio, P., Faraggiana, R., & Sbordone, L. 2005, *A&A*, 436, L9
- Castelli, F., & Kurucz, R. L., 2003, *Proceed. of IAU Symp. 210, Modelling of Stellar Atmospheres*, eds. N. Piskunov et al., poster A20 on the enclosed CD-ROM (astro-ph/0405087)
- Chou, M.-Y., et al. 2006, *ArXiv Astrophysics e-prints*, arXiv:astro-ph/0605101
- Cohen, J. G. 2004, *AJ*, 127, 1545
- Cowley, C.R. & Corliss, C.H. 1983, *MNRAS* 203, 651 (log gf: CC)
- Den Hartog, E. A., Lawler, J. E., Sneden, C., & Cowan, J. J. 2003, *ApJS*, 148, 543 (log gf: HA)
- Edvardsson, B., Andersen, J., Gustafsson, B., Lambert, D. L., Nissen, P. E., & Tomkin, J. 1993, *A&A*, 275, 101 (log gf: ED)
- Fuhr, J.R., Martin, G.A., and Wiese, W.L. 1988. *J.Phys.Chem.Ref.Data* 17, Suppl. 4 (log gf: FMW)
- Garz, T. 1973, *A&A*, 26, 471. (log gf: GARZ)
- Girardi, L., Bertelli, G., Bressan, A., Chiosi, C., Groenewegen, M. A. T., Marigo, P., Salasnich, B., & Weiss, A. 2002, *A&A*, 391, 195
- Gratton, R. G., Carretta, E., Desidera, S., Lucatello, S., Mazzei, P., & Barbieri, M. 2003, *A&A*, 406, 131 (log gf: GC)
- Gratton, R. G., Carretta, E., Eriksson, K., & Gustafsson, B. 1999, *A&A*, 350, 955
- Hannaford, P., Lowe, R. M., Grevesse, N., & Noels, A. 1992, *A&A*, 259, 301 (log gf: H92)
- Hannaford, P., Lowe, R.M., Grevesse, N., Biemont, E., & Whaling, W. 1982, *ApJ* 261, 736 (log gf: HL)
- Helmi, A., & White, S. D. M. 1999, *MNRAS*, 307, 495
- Hill, V., Andrievsky, S., & Spite, M. 1995, *A&A*, 293, 347 (log gf: H)
- Ibata, R. A., Gilmore, G., & Irwin, M. J. 1994, *Nature*, 370, 194
- Ibata, R. A., Gilmore, G., & Irwin, M. J. 1995, *MNRAS*, 277, 781
- Ibata, R. A., Wyse, R. F. G., Gilmore, G., Irwin, M. J., & Suntzeff, N. B. 1997, *AJ*, 113, 634
- Johansson, S., Litzén, U., Lundberg, H., & Zhang, Z. 2003, *ApJ*, 584, L107
- Kurucz, R., L., & Peytremann, E. 1975, *SAO Special Report* 362 (log gf: KP)
- Kurucz, R.L. 1988, *Trans. IAU, XXB*, M. McNally, ed., Dordrecht: Kluwer, 168-172 (log gf: K88)
- Kurucz R. L., 1993, *CDROM* 13, 18
- Kurucz, R. L. 2005, *Memorie della Societa Astronomica Italiana Supplement*, 8, 14
- Lanfranchi, G. A., & Matteucci F., 2003, *MNRAS*, 345, 71
- Lanfranchi, G. A., & Matteucci F., 2004, *MNRAS*, 351, 1338
- Lanfranchi, G. A., Matteucci, F., & Cescutti, G. 2006, *MNRAS*, 365, 477
- Lanfranchi, G. A., Matteucci F., & Cescutti, G., 2005, *astro-ph/0603577* (2006B)
- Laurent, J. and Weniger, S. 1970, *JQSRT* 10, 315 (log gf: LW)
- Lawler, J. E., Bonvallet, G., & Sneden, C. 2001, *ApJ*, 556, 452 (log gf: LA)
- Layden, A. C., & Sarajedini, A. 2000, *AJ*, 119, 1760
- Majewski, S. R., Skrutskie, M. F., Weinberg, M. D., & Ostheimer, J. C. 2003, *ApJ*, 599, 1082
- Marconi, G., Buonanno, R., Castellani, M., Iannicola, G., Molaro, P., Pasquini, L., & Pulone, L. 1998, *A&A*, 330, 453
- Martin, G.A., Fuhr, J.R., and Wiese, W.L. 1988. *J.Phys.Chem.Ref.Data* 17, Suppl. 3 (log gf: MFW)
- McWilliam, A., & Smecker-Hane, T. A. 2005, *ASP Conf. Ser. 336: Cosmic Abundances as Records of Stellar Evolution and Nucleosynthesis*, 336, 221 (2005 B)
- McWilliam, A., & Smecker-Hane, T. A. 2005, *ApJ*, 622, L29
- McWilliam, A., Rich, R. M., & Smecker-Hane, T. A. 2003, *ApJ*, 593, L145 (2003 B)
- McWilliam, A., Rich, R. M., & Smecker-Hane, T. A. 2003, *ApJ*, 592, L21
- Meggers, W.F, Corliss, C.H. & Scribner, B.F. 1975, *NBS Monograph* 145 (log gf: MC')
- Miles, B.M. & Wiese, W.L. 1969, *NBS Technical Note* 474 (log gf: NBS for Ba)
- Monaco, L., Bellazzini, M., Ferraro, F. R., & Pancino, E. 2005, *MNRAS*, 356, 1396 (2005B)
- Monaco, L., Bellazzini, M., Ferraro, F. R., & Pancino, E. 2004, *MNRAS*, 353, 874
- Monaco, L., Ferraro, F. R., Bellazzini, M., & Pancino, E. 2002, *ApJ*, 578, L47
- Monaco, L., Bellazzini, M., Bonifacio, P., Ferraro, F. R., Marconi, G., Pancino, E., Sbordone, L., & Zaggia, S. 2005, *A&A*, 441, 141
- Pritzl, B. J., Venn, K. A., & Irwin, M. 2005, *AJ*, 130, 2140
- Reddy, B. E., Lambert, D. L., & Allende Prieto, C. 2006, *MNRAS*, 343
- Reddy, B. E., Tomkin, J., Lambert, D. L., & Allende Prieto, C. 2003, *MNRAS*, 340, 304
- Sbordone, L., Bonifacio, P., Marconi, G., Buonanno, R., & Zaggia, S. 2005, *A&A*, 437, 905
- Sbordone, L. 2005, *Memorie della Societa Astronomica Italiana Supplement*, 8, 61 (2005B)
- Sbordone, L., Bonifacio, P., Castelli, F., & Kurucz, R. L. 2004, *Memorie della Societa Astronomica Italiana Supplement*, 5, 93
- Schlegel, D. J., Finkbeiner, D. P., & Davis, M. 1998, *ApJ*, 500, 525
- Smith, G. & Raggett, D. S. J. 1981, *Journal of Physics & Atomic Molecular Physics*, 14, 4015 (log gf: SR)
- Shetrone, M., Venn, K. A., Tolstoy, E., Primas, F., Hill, V., & Kaufer, A. 2003, *AJ*, 125, 684
- Shetrone, M. D., Côté, P., & Sargent, W. L. W. 2001, *ApJ*, 548, 592

- Storey, P. J., & Zeippen, C. J. 2000, MNRAS, 312, 813 (log gf: STZ)
- Tautvaišienė, G., Wallerstein, G., Geisler, D., Gonzalez, G., & Charbonnel, C. 2004, AJ, 127, 373
- Venn, K. A., Irwin, M., Shetrone, Tout, C. A., Hill, V., & Tolstoy, E., 2004, AJ, 128, 1177
- Vladilo, G., Sbordone, L., & Bonifacio, P. 2003, The Local Group as an Astrophysical Laboratory, 107
- Wiese, W.L., Smith, M.W., and Miles, B.M. 1969, NSRDS-NBS 22 (log gf: NBS for Al, S and Ca)
- Wiese, W.L. & Fuhr, J.R. 1975, J.Phys.Chem.Ref.Data 4, 263 (log gf: NBS for Sc)
- Zaggia, S., et al. 2004, Memorie della Societa Astronomica Italiana Supplement, 5, 291

Table 4. Absolute abundances, assumed solar abundances, [Fe/H], [X/Fe] values and associated errors for Sgr dSph main body stars # 432 # to 716. The upper panel hosts assumed solar abundances and absolute measured abundances for the sample stars. The published error is simply the RMS of the measured lines, thus is absent for species where a single line has been used. The lower panel lists [X/Fe I] ratios for the neutral species, [X/Fe II] ratios for the ionized ones. [O/Fe II] is listed instead of [O/Fe I] due to the strong gravity sensitivity of [O I] 630.03 nm line. Iron values are [Fe/H] under Fe I and [Fe II/Fe I] under Fe II.

	Sun	432		628		635		656		709		716	
	A(X)	A(X)	σ	A(X)	σ	A(X)	σ	A(X)	σ	A(X)	σ	A(X)	σ
O I	8.72	8.03	–	8.35	–	8.33	–	8.15	–	8.50	–	8.54	–
Na I	6.33	–	–	5.81	0.08	5.40	0.03	5.74	0.08	6.03	0.13	5.83	0.16
Mg I	7.58	6.64	0.01	7.16	0.12	7.10	0.13	6.99	0.04	7.21	0.12	7.13	0.02
Al I	6.47	–	–	–	–	–	–	–	–	–	–	5.61	–
Si I	7.55	6.66	0.17	7.30	0.10	7.12	0.11	7.25	0.08	7.37	0.14	7.39	0.15
Ca I	6.36	5.48	0.08	5.83	0.15	5.80	0.09	5.96	0.18	6.13	0.16	5.97	0.12
Sc II	3.17	2.04	–	2.20	–	2.45	–	2.34	–	2.72	–	2.58	–
Ti I	5.02	4.01	0.08	4.44	0.15	4.13	0.14	4.44	0.12	4.59	0.21	4.38	0.12
V I	4.00	–	–	3.35	0.16	3.06	0.08	3.38	0.04	3.47	0.15	3.52	0.03
Cr II	5.67	–	–	–	–	5.31	–	5.45	–	5.64	–	5.78	–
Mn I	5.39	4.20	–	4.83	–	4.60	–	4.75	–	5.03	–	4.94	–
Fe I	7.50	6.61	0.12	7.22	0.13	7.14	0.12	7.13	0.12	7.52	0.12	7.35	0.16
Fe II	7.50	6.67	0.12	7.23	0.11	7.19	0.17	7.12	0.19	7.59	0.13	7.40	0.13
Co I	4.92	3.69	0.15	4.15	0.06	4.02	0.13	4.07	0.06	4.16	0.02	4.30	0.06
Ni I	6.25	4.91	0.01	5.61	0.08	5.44	0.15	5.51	0.10	5.83	0.17	5.71	0.12
Cu I	4.21	2.29	–	3.06	–	3.05	–	3.05	–	3.43	–	3.17	–
Zn I	4.60	3.45	–	–	–	–	–	3.92	–	3.91	–	3.99	–
Y II	2.24	0.88	0.11	1.73	0.15	1.64	0.05	1.68	0.16	2.09	0.03	1.96	0.05
Ba II	2.13	1.49	–	2.27	–	1.78	–	2.20	–	2.85	–	2.11	–
La II	1.13	0.50	0.14	1.74	0.02	1.16	0.25	1.33	0.15	2.16	0.12	1.82	0.22
Ce II	1.58	0.78	–	1.58	0.02	1.48	0.09	1.29	0.06	2.11	0.21	1.89	0.13
Nd II	1.50	0.84	0.22	1.63	0.20	1.34	0.17	1.47	0.13	2.03	0.17	1.80	0.24

	432		628		635		656		709		716	
	[X/Fe]	σ	[X/Fe]	σ	[X/Fe]	σ	[X/Fe]	σ	[X/Fe]	σ	[X/Fe]	σ
[O I/Fe II]	0.14	–	-0.10	–	-0.08	–	-0.19	–	-0.31	–	-0.08	–
Na I	–	–	-0.24	0.15	-0.57	0.12	-0.22	0.14	-0.32	0.18	-0.35	0.23
Mg I	-0.05	0.12	-0.14	0.18	-0.12	0.18	-0.22	0.13	-0.39	0.17	-0.30	0.16
Al I	–	–	–	–	–	–	–	–	–	–	-0.71	–
Si I	0.00	0.21	0.03	0.16	-0.07	0.16	0.07	0.14	-0.20	0.18	-0.01	0.22
Ca I	0.01	0.14	-0.25	0.20	-0.20	0.15	-0.03	0.22	-0.25	0.20	-0.24	0.20
Sc II	-0.30	–	-0.70	–	-0.41	–	-0.45	–	-0.54	–	-0.49	–
Ti I	-0.12	0.14	-0.30	0.20	-0.53	0.18	-0.21	0.17	-0.45	0.24	-0.49	0.20
V I	–	–	-0.37	0.21	-0.58	0.14	-0.25	0.13	-0.55	0.19	-0.33	0.16
Cr II	–	–	–	–	-0.05	–	0.16	–	-0.12	–	0.21	–
Mn I	-0.30	–	-0.28	–	-0.43	–	-0.27	–	-0.38	–	-0.30	–
[Fe I/H]	-0.89	0.12	-0.28	0.13	-0.36	0.12	-0.37	0.12	0.02	0.12	-0.15	0.16
[Fe II/Fe I]	0.06	0.17	0.01	0.17	0.05	0.21	-0.01	0.22	0.07	0.18	0.16	0.05
Co I	-0.34	0.19	-0.49	0.14	-0.54	0.18	-0.48	0.13	-0.78	0.12	-0.47	0.17
Ni I	-0.45	0.12	-0.36	0.15	-0.45	0.19	-0.37	0.16	-0.44	0.21	-0.39	0.20
Cu I	-1.03	–	-0.87	–	-0.80	–	-0.79	–	-0.80	–	-0.89	–
Zn I	-0.26	–	–	–	–	–	-0.31	–	-0.71	–	-0.46	–
Y II	-0.53	0.16	-0.24	0.19	-0.29	0.18	-0.18	0.25	-0.24	0.13	-0.18	0.14
Ba II	0.19	–	0.41	–	-0.04	–	0.45	–	0.63	–	0.08	–
La II	0.20	0.18	0.88	0.11	0.34	0.30	0.58	0.24	0.94	0.18	0.79	0.26
Ce II	0.03	–	0.27	0.11	0.21	0.19	0.09	0.20	0.44	0.25	0.41	0.18
Nd II	0.17	0.25	0.40	0.23	0.15	0.24	0.35	0.23	0.44	0.21	0.40	0.27

Table 5. Same as in table 4 for stars # 717 to 927.

	Sun	717		772		867		879		894		927	
	A(X)	A(X)	σ	A(X)	σ	A(X)	σ	A(X)	σ	A(X)	σ	A(X)	σ
O I	8.72	8.49	–	8.07	–	8.01	–	–	–	8.33	–	8.45	–
Na I	6.33	5.87	0.16	5.52	0.15	5.36	0.07	5.64	0.08	5.82	0.10	6.00	0.14
Mg I	7.58	7.33	0.05	6.85	0.13	6.76	0.11	6.96	0.13	6.98	0.16	7.08	0.09
Al I	6.47	5.66	–	–	–	–	–	5.76	–	–	–	5.70	–
Si I	7.55	7.51	0.14	7.18	0.12	6.96	0.15	6.98	0.03	7.41	0.07	7.40	0.08
Ca I	6.36	6.18	0.19	5.68	0.16	5.63	0.19	5.74	0.21	5.96	0.18	5.99	0.16
Sc II	3.17	3.12	–	2.27	0.13	1.90	–	2.32	0.07	2.30	–	2.71	–
Ti I	5.02	4.41	0.17	4.13	0.12	4.14	0.10	4.45	0.12	4.52	0.13	4.40	0.19
V I	4.00	3.39	0.15	3.06	–	–	–	–	–	3.42	0.22	3.52	0.11
Cr II	5.67	5.86	–	5.24	–	–	–	5.30	–	5.02	–	5.74	–
Mn I	5.39	4.91	–	4.56	–	–	–	4.80	–	4.87	–	4.79	–
Fe I	7.50	7.44	0.10	6.99	0.12	6.74	0.17	7.01	0.14	7.18	0.14	7.26	0.14
Fe II	7.50	7.53	0.16	7.02	0.03	6.70	0.10	7.13	0.07	7.17	0.15	7.30	0.08
Co I	4.92	4.20	–	3.90	0.05	3.68	0.05	4.09	0.07	4.25	0.02	4.31	0.08
Ni I	6.25	5.72	0.12	5.49	0.11	5.07	0.20	5.43	0.12	5.44	0.08	5.58	0.13
Cu I	4.21	3.17	–	3.02	–	2.86	–	2.98	–	3.38	–	3.49	–
Zn I	4.60	4.26	–	–	–	3.44	–	–	–	3.50	–	3.94	–
Y II	2.24	1.97	0.15	1.30	0.12	0.85	0.22	1.42	0.04	1.51	0.31	1.84	0.04
Ba II	2.13	2.74	–	2.05	–	1.03	–	2.21	–	2.16	–	2.46	–
La II	1.13	1.47	0.10	1.03	0.04	0.49	–	1.00	0.10	1.14	0.09	1.52	0.02
Ce II	1.58	1.69	0.14	1.29	0.11	0.91	0.03	1.48	0.07	1.44	0.07	1.82	0.14
Nd II	1.50	1.78	0.20	1.08	0.14	0.59	0.11	1.23	0.16	1.38	0.10	2.08	0.22

	717		772		867		879		894		927	
	[X/Fe]	σ	[X/Fe]	σ	[X/Fe]	σ	[X/Fe]	σ	[X/Fe]	σ	[X/Fe]	σ
[O I/Fe II]	-0.26	–	-0.17	–	0.09	–	–	–	-0.06	–	-0.07	–
Na I	-0.40	0.19	-0.30	0.19	-0.21	0.18	-0.20	0.16	-0.19	0.17	-0.09	0.20
Mg I	-0.19	0.11	-0.22	0.18	-0.06	0.20	-0.13	0.19	-0.28	0.21	-0.26	0.17
Al I	-0.75	–	–	–	–	–	-0.22	–	–	–	-0.53	–
Si I	0.02	0.17	0.14	0.17	0.17	0.23	-0.08	0.14	0.18	0.16	0.09	0.16
Ca I	-0.12	0.21	-0.17	0.20	0.03	0.25	-0.13	0.25	-0.08	0.23	-0.13	0.21
Sc II	-0.08	–	-0.42	0.13	-0.47	–	-0.48	0.10	-0.54	–	-0.26	–
Ti I	-0.55	0.20	-0.38	0.17	-0.12	0.20	-0.08	0.18	-0.18	0.19	-0.38	0.24
V I	-0.55	0.18	-0.43	–	–	–	–	–	-0.26	0.26	-0.24	0.18
Cr II	0.16	–	0.05	–	–	–	–	–	-0.32	–	0.27	–
Mn I	-0.42	–	-0.32	–	–	–	-0.10	–	-0.20	–	-0.36	–
[Fe I/H]	-0.06	0.10	-0.51	0.12	-0.76	0.17	-0.49	0.14	-0.32	0.14	-0.24	0.14
[Fe II/Fe I]	0.09	0.19	0.03	0.12	-0.04	0.20	0.12	0.16	-0.01	0.21	0.04	0.16
Co I	-0.66	–	-0.51	0.13	-0.48	0.18	-0.34	0.16	-0.35	0.14	-0.37	0.16
Ni I	-0.47	0.16	-0.25	0.16	-0.42	0.26	-0.33	0.18	-0.49	0.16	-0.43	0.19
Cu I	-0.98	–	-0.68	–	-0.59	–	-0.74	–	-0.51	–	-0.48	–
Zn I	-0.28	–	–	–	-0.40	–	–	–	-0.78	–	-0.42	–
Y II	-0.30	0.22	-0.46	0.12	-0.59	0.24	-0.45	0.08	-0.40	0.34	-0.20	0.09
Ba II	0.58	–	0.40	–	-0.30	–	0.45	–	0.36	–	0.53	–
La II	0.31	0.19	0.38	0.05	0.16	–	0.24	0.12	0.34	0.17	0.59	0.08
Ce II	0.08	0.21	0.19	0.11	0.13	0.10	0.27	0.10	0.19	0.17	0.44	0.16
Nd II	0.25	0.26	0.06	0.14	-0.11	0.15	0.10	0.17	0.21	0.18	0.78	0.23

Table 6. Same as in table 4 but now for Terzan 7 stars.

	Sun	1272		1282		1515		1665		1708	
	A(X)	A(X)	σ	A(X)	σ	A(X)	σ	A(X)	σ	A(X)	σ
O I	8.72	8.17	–	8.36	–	–	–	8.43	–	8.34	–
Na I	6.33	5.49	0.02	5.48	0.06	5.42	0.04	5.49	0.07	5.32	0.04
Mg I	7.58	6.88	0.13	6.88	0.05	6.99	0.09	6.93	0.12	6.84	0.08
Al I	6.47	5.55	0.11	5.47	0.01	5.66	–	5.43	0.02	5.43	–
Si I	7.55	6.91	0.16	7.06	0.11	7.14	0.05	7.00	0.12	6.98	0.20
S I	7.21	–	–	6.62	0.04	–	–	6.62	0.04	6.59	0.04
Ca I	6.36	5.88	0.09	5.74	0.09	5.85	0.10	5.79	0.11	5.65	0.05
Sc II	3.17	2.15	0.01	2.36	0.04	2.42	0.04	2.30	0.04	2.29	0.15
Ti I	5.02	4.47	0.09	4.50	0.13	4.52	0.07	4.59	0.21	4.39	0.11
V I	4.00	3.35	0.16	3.35	0.03	3.43	0.04	3.43	0.07	3.20	0.03
Cr I	5.67	4.99	0.02	5.05	0.04	5.02	0.04	5.17	0.08	5.03	0.09
Mn I	5.39	4.47	–	4.58	–	4.45	–	–	–	–	–
Fe I	7.50	6.83	0.08	6.96	0.11	6.94	0.09	6.99	0.14	6.94	0.12
Fe II	7.50	6.85	0.06	6.92	0.10	6.89	0.08	6.98	0.09	6.96	0.06
Co I	4.92	4.11	0.12	4.27	0.09	4.25	0.09	4.10	–	4.01	–
Ni I	6.25	5.32	0.09	5.47	0.08	5.54	0.05	5.49	0.13	5.52	0.11
Cu I	4.21	3.14	–	2.91	–	3.22	–	–	–	–	–
Zn I	4.60	3.39	–	3.88	–	3.81	–	–	–	–	–
Y II	2.24	1.18	0.11	1.42	0.19	1.61	0.13	1.79	–	1.47	–
Ba II	2.13	1.81	–	2.01	–	2.09	–	–	–	1.90	–
La II	1.13	0.85	0.07	1.15	0.21	1.07	0.10	1.09	0.18	0.88	0.10
Ce II	1.58	1.03	0.11	1.27	0.14	1.51	0.11	–	–	–	–
Nd II	1.50	1.07	0.10	1.40	0.19	1.47	0.21	–	–	–	–

	1272		1282		1515		1665		1708	
	[X/Fe]	σ	[X/Fe]	σ	[X/Fe]	σ	[X/Fe]	σ	[X/Fe]	σ
[O I/Fe II]	0.10	–	0.22	–	–	–	0.23	–	0.16	–
Na I	-0.17	0.08	-0.31	0.13	-0.35	0.10	-0.33	0.16	-0.45	0.13
Mg I	-0.03	0.15	-0.16	0.12	-0.03	0.13	-0.14	0.18	-0.18	0.14
Al I	-0.25	0.14	-0.46	0.11	-0.25	–	-0.53	0.14	-0.48	–
Si I	0.03	0.18	0.05	0.16	0.15	0.10	-0.04	0.18	-0.01	0.23
S I	–	–	-0.05	0.12	–	–	-0.08	0.15	-0.06	0.13
Ca I	0.19	0.12	-0.08	0.14	0.05	0.13	-0.06	0.18	-0.15	0.13
Sc II	-0.37	0.06	-0.23	0.11	-0.14	0.09	-0.35	0.10	-0.34	0.16
Ti I	0.12	0.12	0.02	0.17	0.06	0.11	0.08	0.25	-0.07	0.16
V I	0.02	0.18	-0.11	0.11	-0.01	0.10	-0.06	0.16	-0.24	0.12
Cr I	-0.01	0.08	-0.08	0.12	-0.09	0.10	0.01	0.16	-0.08	0.15
Mn I	-0.25	–	-0.27	–	-0.38	–	–	–	–	–
[Fe I/H]	-0.67	0.08	-0.54	0.11	-0.56	0.09	-0.51	0.14	-0.56	0.12
[Fe II/Fe I]	0.02	0.10	-0.04	0.15	-0.05	0.12	-0.01	0.17	0.02	0.13
Co I	-0.14	0.14	-0.11	0.14	-0.11	0.13	-0.31	–	-0.35	–
Ni I	-0.26	0.12	-0.24	0.14	-0.15	0.10	-0.25	0.19	-0.17	0.16
Cu I	-0.40	–	-0.76	–	-0.43	–	–	–	–	–
Zn I	-0.54	–	-0.18	–	-0.23	–	–	–	–	–
Y II	-0.41	0.13	-0.24	0.21	-0.02	0.15	0.07	–	-0.23	–
Ba II	0.33	–	0.46	–	0.57	–	–	–	0.31	–
La II	0.37	0.09	0.60	0.23	0.55	0.13	0.48	0.20	0.29	0.12
Ce II	0.10	0.13	0.27	0.17	0.54	0.14	–	–	–	–
Nd II	0.22	0.12	0.48	0.21	0.58	0.22	–	–	–	–

Online Material

Table .1. Employed lines, $\log gf$ values, $\log gf$ sources, observed EW and derived abundances for Sgr dSph main body stars # 432 to # 716. Codes for the source of the $\log gf$ can be found in the bibliography, NIST code referst to $\log gf$ derived from the NIST online database. For lines that have been synthesized, “syn” substitutes the EW; for lines which have been synthesized by using HFS, $\log gf$ is not provided, substituted by “HFS”, and wavelength is truncated to 0.1 nm. Pure LTE abundances, without NLTE corrections, are published here for Na lines.

Ion	λ (nm)	$\log gf$	source of $\log gf$	EW (pm) 432	A(X)	EW (pm) 628	A(X)	EW (pm) 635	A(X)	EW (pm) 656	A(X)	EW (pm) 709	A(X)	EW (pm) 716	A(X)
O I	630.0304	-9.717	STZ	syn	8.03	syn	8.35	syn	8.33	syn	8.15	syn	8.50	syn	8.54
Na I	568.2633	-0.700	KP	–	–	10.67	5.79	7.56	5.33	9.61	5.76	11.23	6.06	11.18	5.94
Na I	615.4227	-1.560	KP	–	–	4.38	5.72	1.95	5.21	3.36	5.62	–	–	2.47	5.44
Na I	616.0747	-1.260	KP	–	–	5.26	5.56	3.60	5.26	4.34	5.49	6.07	5.74	5.77	5.69
Mg I	552.8405	-0.552	GC	–	–	21.74	7.00	22.55	7.07	19.77	6.96	21.53	7.17	21.90	7.14
Mg I	571.1087	-1.729	GC	7.98	6.63	12.46	7.12	10.81	6.92	11.05	7.04	10.66	7.05	11.76	7.10
Mg I	631.8716	-1.945	GC	2.08	6.65	5.04	7.16	5.83	7.28	3.59	6.98	5.95	7.39	4.53	7.14
Mg I	631.9237	-2.165	GC	–	–	4.77	7.34	3.66	7.15	–	–	3.61	7.22	–	–
Al I	669.8673	-1.647	NBS	–	–	–	–	–	–	–	–	–	–	1.90	5.60
Si I	577.2147	-1.750	GARZ	–	–	–	–	–	–	–	–	4.82	7.27	–	–
Si I	594.8541	-1.230	GARZ	6.16	6.81	8.42	7.14	8.26	7.21	9.30	7.35	8.84	7.49	10.26	7.56
Si I	612.5021	-1.540	ED	1.80	6.82	4.10	7.37	–	–	3.72	7.31	2.29	7.12	4.03	7.44
Si I	614.2482	-1.480	ED	–	–	4.54	7.40	3.21	7.18	3.50	7.21	4.34	7.52	3.31	7.24
Si I	614.5015	-1.430	ED	1.39	6.58	–	–	3.28	7.15	3.34	7.12	3.79	7.36	5.14	7.53
Si I	615.5134	-0.770	ED	3.27	6.42	8.26	7.28	5.64	6.93	7.99	7.28	7.87	7.48	7.01	7.19
Ca I	551.2980	-0.447	SR	–	–	10.74	5.86	10.64	5.91	10.69	6.04	10.47	6.07	11.31	6.05
Ca I	560.1277	-0.523	SR	–	–	–	–	–	–	13.80	6.35	–	–	–	–
Ca I	585.7451	0.240	SR	10.56	5.52	15.85	5.99	14.22	5.84	14.22	5.95	–	–	15.84	6.09
Ca I	586.7562	-1.490	GC	1.49	5.42	3.86	5.77	3.22	5.61	4.26	5.92	4.68	5.98	–	–
Ca I	612.2217	-0.315	NIST	14.17	5.45	–	–	19.53	5.82	19.56	6.00	19.51	6.08	22.15	6.22
Ca I	615.6022	-2.180	NIST	–	–	–	–	–	–	–	–	–	–	–	–
Ca I	616.1296	-1.266	SR	5.98	5.58	–	–	9.33	5.94	9.98	6.20	10.46	6.37	9.85	6.07
Ca I	616.2174	0.100	NBS	–	–	–	–	–	–	–	–	–	–	–	–
Ca I	616.6438	-1.142	SR	6.75	5.60	10.81	6.03	9.54	5.85	9.73	6.03	10.29	6.20	9.91	5.95
Ca I	616.9042	-0.797	SR	7.25	5.36	13.05	6.08	10.88	5.77	11.64	6.05	12.11	6.25	11.75	5.94
Ca I	616.9562	-0.270	NBS	–	–	–	–	–	–	–	–	–	–	–	–
Ca I	643.9075	0.390	SR	13.16	5.40	18.30	5.74	17.94	5.78	17.69	5.89	18.91	6.14	19.22	5.99
Ca I	645.5597	-1.290	SR	5.86	5.57	8.98	5.84	8.05	5.71	8.16	5.87	8.02	5.86	8.84	5.89
Ca I	649.3781	-0.109	SR	11.35	5.54	15.17	5.74	15.03	5.83	13.98	5.78	–	–	15.20	5.83
Ca I	649.9650	-0.818	SR	7.69	5.47	10.77	5.67	10.91	5.77	10.92	5.90	12.82	6.37	11.51	5.87
Ca I	650.8850	-2.110	NBS	1.38	5.38	2.48	5.61	–	–	2.01	5.57	–	–	3.29	5.84
Ca I	679.8479	-2.320	K88	–	–	–	–	–	–	1.45	5.81	2.28	6.01	–	–
Sc II	552.6790	0.130	MFW	8.28	2.04	9.87	2.19	10.42	2.45	10.01	2.34	9.97	2.72	10.74	2.58
Sc II	632.0852	-1.770	NBS	–	–	–	–	–	–	–	–	–	–	–	–
Ti I	488.5078	0.358	MFW	7.06	4.12	10.22	4.38	–	–	9.83	4.56	–	–	–	–
Ti I	491.5229	-1.019	MFW	–	–	3.98	4.65	–	–	1.91	4.32	3.13	4.56	–	–
Ti I	499.7097	-2.118	MFW	5.51	3.88	9.23	4.21	7.97	3.95	8.42	4.31	7.85	4.20	8.88	4.28
Ti I	508.7058	-0.780	MFW	–	–	7.95	4.47	5.73	4.05	6.16	4.33	8.29	4.78	5.84	4.23
Ti I	586.6450	-0.840	MFW	6.43	4.03	10.31	4.35	9.16	4.16	9.91	4.53	10.26	4.65	10.61	4.52
Ti I	612.6215	-1.425	MFW	3.45	4.01	8.28	4.57	6.99	4.33	7.18	4.58	8.17	4.75	7.03	4.48
V I	573.7059	-0.740	MFW	–	–	5.48	3.49	3.80	3.14	3.79	3.36	4.87	3.49	5.28	3.57
V I	613.5361	-0.746	MFW	–	–	3.49	3.14	3.14	2.98	3.92	3.34	3.92	3.28	5.35	3.52
V I	615.0157	-1.780	MFW	–	–	4.87	3.43	–	–	3.93	3.43	5.68	3.64	4.57	3.49
Cr II	488.4607	-2.080	MFW	–	–	–	–	3.59	5.31	4.55	5.45	4.14	5.64	5.53	5.78
Mn I	511.79**	-1.140	MFW	HFS	4.20	HFS	4.83	HFS	4.60	HFS	4.75	HFS	5.03	HFS	4.94
Fe I	489.2859	-1.290	FMW	4.42	6.65	8.28	7.22	–	–	7.78	7.28	7.84	7.49	8.67	7.44
Fe I	506.7151	-0.970	FMW	–	–	10.54	7.34	8.42	7.01	9.54	7.34	9.52	7.56	–	–
Fe I	510.4438	-1.690	FMW	2.46	6.46	–	–	4.51	7.02	4.81	7.15	6.28	7.56	7.28	7.62
Fe I	510.9652	-0.980	FMW	6.07	6.78	9.90	7.29	9.51	7.33	7.98	7.07	10.01	7.67	8.58	7.16
Fe I	552.5545	-1.330	FMW	3.51	6.46	7.17	7.01	8.14	7.26	7.92	7.29	7.43	7.35	8.83	7.44
Fe I	585.5076	-1.760	FMW	–	–	4.43	7.42	3.57	7.26	–	–	5.02	7.70	4.70	7.56
Fe I	585.6087	-1.640	FMW	2.38	6.57	6.16	7.21	5.52	7.13	4.85	7.08	6.61	7.54	7.65	7.59
Fe I	585.8779	-2.260	FMW	–	–	2.56	7.10	2.88	7.15	2.00	7.01	–	–	2.89	7.27
Fe I	586.1109	-2.450	FMW	–	–	–	–	–	–	–	–	2.84	7.54	1.60	7.20
Fe I	587.7794	-2.230	FMW	1.65	6.81	4.49	7.38	3.84	7.26	3.64	7.31	4.44	7.53	3.73	7.35
Fe I	588.3817	-1.360	FMW	5.80	6.64	10.41	7.28	–	–	8.48	7.08	8.85	7.36	10.38	7.42
Fe I	615.1616	-3.299	FMW	6.81	6.58	–	–	–	–	9.37	6.93	–	–	10.86	7.16
Fe I	616.5360	-1.550	FMW	4.19	6.70	–	–	6.22	6.96	6.39	7.07	6.64	7.25	–	–

Fe I	618.7990	-1.720	FMW	4.01	6.59	—	—	7.51	7.12	6.49	7.01	8.42	7.56	8.21	7.31
Fe I	649.6465	-0.570	FMW	3.56	6.35	9.10	7.21	7.73	7.05	7.81	7.12	9.40	7.61	8.50	7.22
Fe I	670.3565	-3.160	FMW	4.09	6.57	7.53	6.99	—	—	7.27	7.09	—	—	7.80	7.16
Fe II	483.3197	-4.780	FMW	1.20	6.67	—	—	—	—	3.18	7.34	3.50	7.72	—	—
Fe II	492.3927	-1.320	FMW	14.99	6.44	—	—	—	—	—	—	—	—	—	—
Fe II	499.3358	-3.650	FMW	4.10	6.53	8.35	7.43	6.35	7.18	7.05	7.22	7.35	7.72	7.14	7.39
Fe II	510.0664	-4.370	FMW	2.08	6.73	3.76	7.23	4.30	7.45	3.30	7.12	3.41	7.47	4.64	7.59
Fe II	513.2669	-4.180	FMW	2.57	6.68	4.43	7.18	4.01	7.19	4.72	7.25	3.81	7.38	4.64	7.40
Fe II	516.1184	-4.483	K88	—	—	—	—	—	—	2.17	7.00	—	—	—	—
Fe II	525.6937	-4.250	K88	2.57	6.85	—	—	3.36	7.21	—	—	3.73	7.53	—	—
Fe II	526.4812	-3.190	FMW	4.84	6.73	7.10	7.21	—	—	4.81	6.76	7.16	7.68	6.25	7.22
Fe II	614.9259	-2.724	K88	3.69	6.75	4.89	7.09	3.55	6.91	—	—	5.67	7.65	—	—
Co I	533.17**	-6.473	K88	HFS	3.79	HFS	4.18	HFS	3.93	HFS	4.11	HFS	4.14	HFS	4.25
Co I	553.07**	-2.060	FMW	HFS	3.58	HFS	4.11	HFS	4.11	HFS	4.03	HFS	4.18	HFS	4.34
Ni I	585.7747	-0.636	K88	—	—	—	—	—	—	—	—	—	—	—	—
Ni I	612.8963	-3.330	FMW	2.48	4.89	6.81	5.59	4.16	5.15	6.24	5.62	5.60	5.65	6.49	5.70
Ni I	613.0130	-0.960	FMW	—	—	3.14	5.77	2.22	5.56	1.96	5.52	2.60	5.807	3.19	5.88
Ni I	617.5360	-0.530	FMW	—	—	5.69	5.58	5.32	5.56	4.71	5.48	6.47	5.99	5.63	5.69
Ni I	617.6807	-0.260	LW	3.27	4.92	7.10	5.55	6.32	5.48	6.75	5.59	7.99	6.06	7.45	5.75
Ni I	617.7236	-3.500	FMW	—	—	4.24	5.54	3.86	5.46	2.78	5.35	3.71	5.65	3.24	5.52
Cu I	510.55**	-1.516	BIEL	HFS	2.29	HFS	3.06	HFS	3.05	HFS	3.05	HFS	3.43	HFS	3.17
Zn I	481.0528	-0.170	BG	5.72	3.45	—	—	—	—	7.88	3.92	6.50	3.91	7.87	3.99
Y II	488.3683	0.070	HL	6.17	0.86	10.65	1.66	9.84	1.67	10.46	1.86	—	—	10.34	1.88
Y II	498.2130	-1.290	HL	—	—	5.81	1.95	3.65	1.59	4.06	1.67	4.43	2.05	4.79	1.98
Y II	508.7417	-0.170	HL	4.93	0.76	9.20	1.54	—	—	7.92	1.43	8.65	2.08	—	—
Y II	511.9113	-1.360	HL	1.71	1.01	4.82	1.78	3.82	1.63	4.41	1.76	4.69	2.13	4.84	2.00
Ba II	649.6896	-0.377	NBS	13.06	1.49	21.52	2.27	15.69	1.78	19.02	2.20	22.13	2.85	17.03	2.11
La II	480.4039	-1.490	LA	—	—	7.18	1.75	—	—	4.55	1.33	6.82	2.28	6.03	1.78
La II	511.4558	-1.030	LA	3.91	0.64	9.46	1.72	7.35	1.41	7.65	1.51	—	—	9.81	2.11
La II	632.0377	-1.610	ABH	1.34	0.36	—	—	2.95	0.90	4.00	1.15	6.73	2.03	5.37	1.56
Ce II	518.7457	0.130	H	1.64	0.78	5.00	1.61	4.45	1.57	2.78	1.21	5.34	2.12	—	—
Ce II	533.0556	-0.360	H	—	—	4.30	1.55	3.30	1.38	3.07	1.35	4.74	2.02	3.94	1.71
Ce II	546.8372	0.140	H	—	—	3.69	1.57	—	—	2.43	1.32	3.51	1.87	4.49	1.94
Ce II	604.3374	-0.430	H	—	—	2.31	1.58	—	—	—	—	3.21	2.44	3.30	2.01
Nd II	491.4382	-0.700	HA	4.53	1.14	8.19	1.80	5.95	1.44	6.80	1.67	7.53	2.33	7.01	1.83
Nd II	495.9119	-0.800	HA	4.17	0.76	9.71	1.83	—	—	—	—	—	—	—	—
Nd II	496.1387	-0.710	MC ⁺	—	—	5.31	1.55	4.78	1.51	4.14	1.40	5.69	2.10	7.19	2.18
Nd II	508.9832	-1.160	MC ⁺	—	—	4.63	1.35	—	—	—	—	5.13	1.86	4.15	1.50
Nd II	529.3162	0.100	HA	3.65	0.63	—	—	5.53	1.06	7.60	1.54	—	—	—	—
Nd II	543.1515	-0.470	HA	—	—	—	—	2.51	1.35	2.24	1.28	3.85	1.96	2.68	1.57
Nd II	548.5695	-0.120	HA	—	—	—	—	—	—	3.79	1.46	4.42	1.91	5.15	1.89

Table 2. As in previous table, for Sgr dSph main body stars # 717 to # 927.

Ion	λ (nm)	$\log gf$	source of $\log gf$	EW (pm) 717	A(X)	EW (pm) 772	A(X)	EW (pm) 867	A(X)	EW (pm) 879	A(X)	EW (pm) 894	A(X)	EW (pm) 927	A(X)
O I	630.0304	-9.717	STZ	syn	8.49	syn	8.07	syn	8.01	–	–	syn	8.33	syn	8.45
Na I	568.2633	-0.700	KP	10.30	5.99	–	–	6.37	5.19	8.22	5.48	10.83	5.86	12.21	6.13
Na I	615.4227	-1.560	KP	2.95	5.57	3.32	5.51	–	–	3.73	5.60	–	–	5.40	5.85
Na I	616.0747	-1.260	KP	4.45	5.54	3.42	5.23	3.50	5.30	4.48	5.43	5.58	5.58	6.19	5.67
Mg I	552.8405	-0.552	GC	–	–	18.19	6.73	17.65	6.62	17.80	6.77	19.47	6.86	19.47	6.95
Mg I	571.1087	-1.729	GC	12.42	7.40	10.16	6.78	10.73	6.84	11.48	7.10	10.49	6.87	11.73	7.14
Mg I	631.8716	-1.945	GC	5.34	7.32	3.19	6.83	2.40	6.69	4.00	7.00	5.32	7.20	4.97	7.19
Mg I	631.9237	-2.165	GC	3.78	7.27	3.24	7.06	2.28	6.88	–	–	–	–	2.96	7.05
Al I	669.8673	-1.647	NBS	2.01	5.66	–	–	–	–	2.88	5.76	–	–	2.64	5.70
Si I	577.2147	-1.750	GARZ	–	–	4.82	7.08	–	–	–	–	–	–	4.82	7.27
Si I	594.8541	-1.230	GARZ	10.14	7.70	8.84	7.23	–	–	7.12	7.02	9.24	7.36	8.98	7.50
Si I	612.5021	-1.540	ED	3.99	7.46	2.29	6.98	–	–	2.30	7.00	3.51	7.30	3.18	7.34
Si I	614.2482	-1.480	ED	3.64	7.33	4.34	7.35	3.87	7.13	2.36	6.96	4.80	7.49	3.63	7.38
Si I	614.5015	-1.430	ED	4.44	7.44	3.79	7.20	3.30	6.98	–	–	4.83	7.44	4.21	7.45
Si I	615.5134	-0.770	ED	8.88	7.63	7.87	7.25	5.99	6.76	5.80	6.95	8.67	7.44	7.88	7.48
Ca I	551.2980	-0.447	SR	11.47	6.37	10.09	5.78	8.98	5.57	–	–	10.24	5.85	12.62	6.34
Ca I	560.1277	-0.523	SR	–	–	12.43	5.87	12.63	5.82	–	–	14.26	6.32	–	–
Ca I	585.7451	0.240	SR	16.28	6.41	13.38	5.66	–	–	12.48	5.69	15.39	6.01	14.65	5.97
Ca I	586.7562	-1.490	GC	4.19	5.96	3.58	5.69	4.00	5.82	4.38	5.86	5.12	5.96	4.98	5.94
Ca I	612.2217	-0.315	NIST	22.05	6.45	17.26	5.53	16.67	5.39	17.26	5.71	21.55	6.02	22.54	6.20
Ca I	615.6022	-2.180	NIST	–	–	–	–	–	–	1.81	5.48	–	–	–	–
Ca I	616.1296	-1.266	SR	–	–	9.20	5.88	8.16	5.73	7.99	5.78	10.72	6.23	8.64	5.85
Ca I	616.2174	0.100	NBS	–	–	–	–	–	–	20.17	5.61	–	–	–	–
Ca I	616.6438	-1.142	SR	10.05	6.27	8.01	5.55	7.21	5.46	10.08	6.09	10.42	6.04	9.61	5.91
Ca I	616.9042	-0.797	SR	11.00	6.14	10.93	5.74	11.18	5.75	9.44	5.61	10.45	5.70	11.73	6.01
Ca I	616.9562	-0.270	NBS	–	–	–	–	–	–	11.45	5.51	–	–	–	–
Ca I	643.9075	0.390	SR	–	–	17.33	5.66	–	–	18.95	6.04	18.43	5.85	17.53	5.82
Ca I	645.5597	-1.290	SR	7.95	5.94	7.85	5.65	8.75	5.82	6.37	5.48	9.46	5.98	9.08	5.93
Ca I	649.3781	-0.109	SR	14.65	6.15	14.52	5.68	13.01	5.34	12.84	5.60	13.99	5.67	14.43	5.80
Ca I	649.9650	-0.818	SR	11.51	6.22	9.95	5.54	–	–	12.01	6.14	11.53	5.90	12.37	6.12
Ca I	650.8850	-2.110	NBS	3.21	5.87	1.51	5.30	–	–	3.28	5.74	–	–	–	–
Ca I	679.8479	-2.320	K88	–	–	2.28	5.93	–	–	–	–	–	–	–	–
Sc II	552.6790	0.130	MFW	12.08	3.12	10.91	2.40	10.54	1.90	9.94	2.40	9.67	2.30	10.31	2.71
Sc II	632.0852	-1.770	NBS	–	–	1.62	2.14	–	–	1.92	2.25	–	–	–	–
Ti I	488.5078	0.358	MFW	–	–	8.97	4.13	9.24	4.18	9.92	4.58	10.63	4.59	8.50	4.15
Ti I	491.5229	-1.019	MFW	–	–	–	–	–	–	–	–	4.72	4.73	2.52	4.30
Ti I	499.7097	-2.118	MFW	–	–	–	–	7.73	4.00	–	–	–	–	–	–
Ti I	508.7058	-0.780	MFW	6.74	4.57	–	–	6.16	4.21	–	–	7.77	4.45	8.42	4.63
Ti I	586.6450	-0.840	MFW	7.41	4.18	8.41	3.99	8.29	4.05	10.14	4.49	10.48	4.45	10.74	4.53
Ti I	612.6215	-1.425	MFW	6.12	4.48	6.72	4.27	5.79	4.26	6.40	4.29	7.06	4.36	–	–
V I	573.7059	-0.740	MFW	2.72	3.18	3.28	3.05	–	–	–	–	6.22	3.57	5.38	3.42
V I	613.5361	-0.746	MFW	4.30	3.44	–	–	–	–	–	–	3.76	3.12	–	–
V I	615.0157	-1.780	MFW	4.41	3.54	–	–	–	–	–	–	6.26	3.58	6.73	3.63
Cr II	488.4607	-2.080	MFW	5.38	5.86	3.76	5.24	–	–	3.76	5.30	2.51	5.02	4.56	5.74
Mn I	511.79**	-1.140	MFW	HFS	4.91	HFS	4.56	HFS	–	HFS	4.80	HFS	4.87	HFS	4.79
Fe I	489.2859	-1.290	FMW	7.21	7.40	5.91	6.78	6.89	6.90	7.09	7.14	8.21	7.31	7.10	7.21
Fe I	506.7151	-0.970	FMW	–	–	8.34	6.92	–	–	7.46	6.89	8.82	7.10	9.00	7.32
Fe I	510.4438	-1.690	FMW	6.32	7.62	–	–	–	–	5.89	7.33	–	–	5.90	7.40
Fe I	510.9652	-0.980	FMW	8.94	7.52	7.90	6.92	8.06	6.86	–	–	9.39	7.31	8.38	7.23
Fe I	552.5545	-1.330	FMW	7.41	7.40	–	–	6.75	6.87	6.25	6.94	7.06	7.05	6.92	7.15
Fe I	585.5076	-1.760	FMW	–	–	–	–	–	–	–	–	–	–	4.09	7.45
Fe I	585.6087	-1.640	FMW	5.86	7.42	6.24	7.22	5.15	6.99	3.85	6.83	6.89	7.39	6.50	7.44
Fe I	585.8779	-2.260	FMW	2.97	7.32	2.37	7.01	–	–	1.97	6.92	2.68	7.11	1.91	6.99
Fe I	586.1109	-2.450	FMW	2.85	7.56	1.22	6.93	–	–	1.81	7.14	2.47	7.33	2.49	7.41
Fe I	587.7794	-2.230	FMW	–	–	3.34	7.14	1.77	6.78	2.74	7.03	–	–	3.94	7.37
Fe I	588.3817	-1.360	FMW	9.18	7.52	9.15	7.07	–	–	7.88	6.97	9.33	7.19	–	–
Fe I	615.1616	-3.299	FMW	–	0.000	–	–	8.04	6.45	9.59	6.95	–	–	–	–
Fe I	616.5360	-1.550	FMW	7.64	7.52	6.46	6.96	4.27	6.56	5.98	6.96	6.58	7.03	6.14	7.06
Fe I	618.7990	-1.720	FMW	6.80	7.25	6.34	6.86	4.92	6.59	7.36	7.16	6.74	6.98	6.69	7.09
Fe I	649.6465	-0.570	FMW	8.07	7.37	8.45	7.12	5.75	6.59	6.26	6.82	9.06	7.31	7.66	7.17
Fe I	670.3565	-3.160	FMW	7.83	7.38	7.16	6.90	7.00	6.85	7.52	7.07	7.61	7.04	8.36	7.31

Fe II	483.3197	-4.780	FMW	—	—	1.94	6.97	—	—	2.72	7.22	—	—	—	—
Fe II	492.3927	-1.320	FMW	—	—	—	—	—	—	—	—	19.57	6.94	20.15	7.22
Fe II	499.3358	-3.650	FMW	6.32	7.37	6.37	7.03	6.96	6.71	5.97	7.06	5.78	7.04	5.47	7.26
Fe II	510.0664	-4.370	FMW	4.13	7.52	—	—	3.63	6.82	—	—	4.34	7.44	—	—
Fe II	513.2669	-4.180	FMW	4.16	7.34	3.98	7.06	4.66	6.83	—	—	4.67	7.33	3.34	7.26
Fe II	516.1184	-4.483	K88	—	—	—	—	—	—	—	—	2.46	7.16	2.12	7.27
Fe II	525.6937	-4.250	K88	5.06	7.74	—	—	3.18	6.71	—	—	2.93	7.09	3.20	7.40
Fe II	526.4812	-3.190	FMW	7.55	7.66	6.09	7.01	6.11	6.58	6.00	7.10	6.32	7.19	5.27	7.25
Fe II	614.9259	-2.724	K88	—	—	—	—	4.42	6.57	—	—	4.80	7.19	4.75	7.45
Co I	533.17**	-6.473	K88	HFS	4.20	HFS	3.86	HFS	3.71	HFS	4.03	HFS	4.23	HFS	4.36
Co I	553.07**	-2.060	FMW	HFS	4.20	HFS	3.94	HFS	3.64	HFS	4.14	HFS	4.25	HFS	4.25
Ni I	585.7747	-0.636	K88	—	—	4.38	5.55	—	—	2.74	5.24	—	—	—	—
Ni I	612.8963	-3.330	FMW	5.34	5.62	5.86	5.39	3.43	4.95	5.60	5.41	5.88	5.46	5.71	5.57
Ni I	613.0130	-0.960	FMW	2.34	5.72	1.88	5.44	—	—	1.89	5.45	1.66	5.40	2.52	5.74
Ni I	617.5360	-0.530	FMW	4.79	5.64	4.93	5.43	4.96	5.35	5.74	5.66	4.10	5.33	3.75	5.38
Ni I	617.6807	-0.260	LW	7.26	5.92	7.86	5.70	3.98	4.91	5.73	5.39	5.98	5.42	—	—
Ni I	617.7236	-3.500	FMW	—	—	3.95	5.43	—	—	3.69	5.41	4.49	5.58	4.13	5.64
Cu I	510.55**	-1.516	BIEL	HFS	3.17	HFS	3.02	HFS	2.86	HFS	2.98	HFS	3.38	HFS	3.49
Zn I	481.0528	-0.170	BG	7.73	4.26	—	—	7.82	3.44	—	—	5.89	3.50	6.70	3.94
Y II	488.3683	0.070	HL	—	—	9.37	1.41	8.15	0.69	—	—	10.54	1.87	—	—
Y II	498.2130	-1.290	HL	3.57	1.79	2.78	1.30	2.93	1.05	3.35	1.47	3.51	1.56	4.01	1.89
Y II	508.7417	-0.170	HL	8.86	2.16	7.13	1.11	6.34	0.58	7.58	1.41	6.12	1.03	8.06	1.78
Y II	511.9113	-1.360	HL	4.20	1.95	3.15	1.39	3.09	1.09	2.91	1.38	3.56	1.58	3.75	1.84
Ba II	649.6896	-0.377	NBS	20.33	2.74	18.92	2.05	15.22	1.03	18.80	2.21	18.96	2.16	18.25	2.46
La II	480.4039	-1.490	LA	3.61	1.37	3.53	0.98	—	—	3.76	1.09	4.18	1.22	4.53	1.54
La II	511.4558	-1.030	LA	—	—	—	—	5.13	0.49	—	—	—	—	—	—
La II	632.0377	-1.610	ABH	4.80	1.57	4.31	1.07	—	—	3.20	0.90	3.65	1.05	4.78	1.50
Ce II	518.7457	0.130	H	4.49	1.86	3.00	1.16	3.06	0.88	4.30	1.51	3.42	1.35	4.50	1.82
Ce II	533.0556	-0.360	H	3.35	1.64	3.26	1.28	—	—	3.53	1.39	3.67	1.46	4.46	1.87
Ce II	546.8372	0.140	H	3.31	1.75	—	—	2.44	0.95	3.60	1.55	3.19	1.50	4.36	2.00
Ce II	604.3374	-0.430	H	1.37	1.48	2.04	1.43	—	—	—	—	—	—	1.63	1.61
Nd II	491.4382	-0.700	HA	5.72	1.80	3.82	0.89	4.51	0.72	5.89	1.45	—	—	6.94	1.99
Nd II	495.9119	-0.800	HA	—	—	6.73	1.17	4.67	0.45	—	—	6.98	1.37	9.28	2.33
Nd II	496.1387	-0.710	MC*	4.76	1.84	3.01	1.04	—	—	2.80	1.03	4.81	1.52	5.53	1.94
Nd II	508.9832	-1.160	MC*	3.54	1.44	2.94	0.94	—	—	3.79	1.17	—	—	—	—
Nd II	529.3162	0.100	HA	—	—	6.48	1.13	5.46	0.59	5.70	1.11	6.30	1.23	9.47	2.36
Nd II	543.1515	-0.470	HA	3.26	1.75	2.84	1.33	—	—	—	—	—	—	3.47	1.80
Nd II	548.5695	-0.120	HA	5.15	2.06	2.32	1.03	—	—	3.53	1.36	3.58	1.41	—	—

Table .3. Same as in previous tables, now for the Ter 7 stars.

Ion	λ (nm)	$\log gf$	source of $\log gf$ (see notes)	EW (pm) 1272	A(X)	EW (pm) 1282	A(X)	EW (pm) 1515	A(X)	EW (pm) 1665	A(X)	EW (pm) 1708	A(X)
O I	630.0304	-9.717	STZ	syn	8.17	syn	8.22	syn	—	syn	8.20	syn	8.24
Na I	498.2814	-0.950	KP	6.21	5.32	7.92	5.36	5.81	5.26	—	—	—	—
Na I	615.4227	-1.560	KP	2.75	5.28	3.50	5.22	2.98	5.35	4.87	5.22	2.60	5.08
Na I	616.0747	-1.260	KP	4.36	5.27	5.67	5.26	4.43	5.30	8.02	5.36	4.81	5.16
Mg I	552.8405	-0.522	GC	20.79	6.88	22.72	6.86	—	—	—	—	—	—
Mg I	571.1087	-1.729	GC	12.14	7.03	12.75	6.96	12.37	7.12	—	—	—	—
Mg I	631.8716	-1.945	GC	2.89	6.68	—	—	3.81	6.91	—	—	4.49	6.88
Mg I	631.9237	-2.165	GC	3.04	6.93	3.30	6.91	2.79	6.93	3.54	6.92	3.31	6.90
Mg I	738.7689	-1.020	KP	—	—	—	—	—	—	4.81	6.82	—	—
Mg I	871.7825	-0.772	GC	—	—	5.40	6.85	—	—	6.41	7.10	4.76	6.73
Mg I	892.3568	-1.659	GC	—	—	4.28	6.84	—	—	—	—	—	—
Al I	669.6022	-1.347	NBS	3.41	5.44	4.64	5.46	—	—	5.98	5.45	4.33	5.43
Al I	669.8673	-1.647	NBS	3.03	5.66	3.00	5.48	2.90	5.66	3.67	5.40	—	—
Si I	594.8541	-1.230	GARZ	—	—	7.32	7.04	8.15	7.23	—	—	—	—
Si I	612.5021	-1.540	ED	3.49	7.16	3.05	7.19	2.76	7.15	—	—	—	—
Si I	613.1852	-1.140	KP	—	—	—	—	—	—	3.68	7.02	—	—
Si I	614.2482	-1.480	ED	2.37	6.87	1.97	6.88	2.70	7.10	1.97	6.92	—	—
Si I	614.5015	-1.430	ED	2.05	6.73	—	—	2.85	7.08	2.17	6.93	—	—
Si I	615.5134	-0.770	ED	5.99	6.89	6.30	7.09	6.43	7.12	5.60	7.06	—	—
Si I	703.4902	-0.880	GARZ	—	—	4.22	7.14	—	—	—	—	5.05	7.22
Si I	725.0627	-1.042	SG	—	—	—	—	—	—	3.45	6.90	3.84	6.83
Si I	727.5292	-1.003	SG	—	—	4.07	6.90	—	—	4.79	7.14	3.99	6.82
Si I	728.9176	-0.197	SG	—	—	—	—	—	—	7.36	6.81	7.96	6.71
Si I	793.2349	-0.470	GARZ	—	—	5.33	7.05	—	—	—	—	5.67	7.03
Si I	874.2446	-0.630	KP	—	—	6.17	7.20	—	—	5.51	7.21	6.88	7.23
S I	921.2863	0.420	NBS	—	—	syn	6.62	—	—	syn	6.62	syn	6.59
S I	922.8093	0.260	NBS	—	—	syn	6.62	—	—	syn	6.62	syn	6.59
S I	923.7538	0.040	NBS	—	—	syn	6.62	—	—	syn	6.62	syn	6.59
Ca I	551.2980	-0.447	SR	11.00	5.90	11.72	5.72	9.85	5.69	—	—	—	—
Ca I	585.7451	0.240	SR	14.37	5.76	—	—	14.75	5.83	—	—	—	—
Ca I	586.7562	-1.490	GC	4.87	5.79	4.73	5.54	4.71	5.78	—	—	—	—
Ca I	616.1296	-1.266	SR	10.22	5.98	—	—	—	—	—	—	—	—
Ca I	616.6438	-1.142	SR	—	—	12.19	5.87	10.97	6.05	13.90	5.90	—	—
Ca I	616.9042	-0.797	SR	12.91	6.05	13.46	5.76	11.89	5.88	15.87	5.93	13.23	5.68
Ca I	643.9075	0.390	SR	18.79	5.80	21.41	5.73	18.69	5.76	—	—	20.87	5.64
Ca I	645.5597	-1.290	SR	—	—	10.88	5.75	9.57	5.90	11.94	5.63	10.31	5.63
Ca I	649.3781	-0.109	SR	16.15	5.87	17.72	5.72	15.70	5.84	19.39	5.71	17.09	5.57
Ca I	649.9650	-0.818	SR	12.17	5.87	13.96	5.81	12.22	5.94	15.41	5.77	13.59	5.70
Sc II	552.6790	0.130	MFW	10.45	2.15	11.21	2.30	10.23	2.43	—	—	—	—
Sc II	624.5637	-0.980	NBS	6.76	2.14	7.90	2.39	6.04	2.36	8.86	2.34	8.76	2.44
Sc II	632.0852	-1.770	NBS	2.69	2.16	3.35	2.39	2.49	2.46	3.70	2.26	2.46	2.14
Ti I	488.5078	0.358	MFW	—	—	—	—	10.72	4.46	—	—	—	—
Ti I	491.5229	-1.019	MFW	5.14	4.58	—	—	4.06	4.44	8.68	4.45	5.49	4.30
Ti I	499.7096	-2.118	MFW	11.51	4.35	14.81	4.58	11.41	4.48	—	—	—	—
Ti I	508.7058	-0.780	MFW	9.36	4.53	—	—	9.19	4.57	—	—	—	—
Ti I	586.6450	-0.840	MFW	11.85	4.37	15.65	4.57	12.41	4.61	—	—	—	—
Ti I	606.4626	-1.944	MFW	—	—	9.61	4.50	—	—	13.38	4.70	9.79	4.53
Ti I	609.2792	-1.379	MFW	—	—	4.73	4.40	—	—	6.88	4.31	3.81	4.28
Ti I	612.6215	-1.425	MFW	9.80	4.52	13.75	4.71	9.32	4.56	—	—	—	—
Ti I	631.2236	-1.552	MFW	—	—	7.91	4.41	—	—	10.52	4.36	6.76	4.27
Ti I	633.6098	-1.743	MFW	—	—	7.34	4.50	—	—	10.38	4.52	6.98	4.47
Ti I	655.6061	-1.074	MFW	—	—	12.51	4.62	—	—	16.40	4.86	10.88	4.35
Ti I	659.9105	-2.085	MFW	—	—	—	—	—	—	15.41	4.83	9.88	4.38
Ti I	686.1447	-0.740	MFW	—	—	4.95	4.27	—	—	7.42	4.25	5.03	4.31
Ti I	718.8565	-1.760	MFW	—	—	7.04	4.37	—	—	—	—	5.73	4.22
Ti I	744.0578	-0.700	MFW	—	—	5.15	4.20	—	—	—	—	4.88	4.19
Ti I	802.4843	-1.140	MFW	—	—	—	—	—	—	—	—	7.61	4.42
Ti I	835.3161	-2.677	MFW	—	—	9.82	4.61	—	—	14.72	4.75	7.99	4.42
Ti I	867.5372	-1.669	MFW	—	—	14.80	4.58	—	—	—	—	14.29	4.49
Ti I	868.2980	-1.941	MFW	—	—	11.91	4.46	—	—	17.32	4.72	11.89	4.46
Ti I	869.2331	-2.295	MFW	—	—	10.48	4.63	—	—	—	—	10.25	4.61
Ti I	873.4712	-2.384	MFW	—	—	9.15	4.56	—	—	14.40	4.74	8.18	4.47
V I	573.7059	-0.740	MFW	7.92	3.56	—	—	6.78	3.45	—	—	—	—
V I	613.5361	-0.746	MFW	6.88	3.32	10.01	3.38	6.63	3.38	13.32	3.50	9.12	3.23

V I	653.1414	-0.840	MFW	4.20	3.18	7.81	3.32	5.37	3.45	11.05	3.36	6.62	3.17
Cr I	633.0090	-2.920	MFW	9.45	4.97	12.41	4.99	8.77	4.98	16.05	5.24	—	—
Cr I	663.0010	-3.560	MFW	5.23	5.02	8.22	5.05	4.95	5.06	11.23	5.05	7.40	4.95
Cr I	735.5960	-0.285	MFW	—	—	12.62	5.09	—	—	15.26	5.22	13.02	5.12
Mn I	511.79**	-1.140	MFW	HFS	4.47	HFS	4.58	HFS	4.45	—	—	—	—
Fe I	466.1535	-1.270	FMW	—	—	4.21	6.68	—	—	6.53	7.07	—	—
Fe I	479.4354	-4.050	FMW	—	—	5.90	6.94	—	—	6.25	6.77	—	—
Fe I	484.9668	-2.680	FMW	—	—	—	—	—	—	—	—	—	—
Fe I	489.2859	-1.290	FMW	7.11	6.923	7.15	6.82	6.51	6.90	—	—	—	—
Fe I	489.6439	-2.050	FMW	—	—	7.20	7.15	—	—	7.80	7.16	—	—
Fe I	491.8013	-1.360	FMW	—	—	6.41	6.75	—	—	6.77	6.73	—	—
Fe I	510.9652	-0.980	FMW	8.24	6.94	—	—	8.24	7.03	—	—	—	—
Fe I	552.5544	-1.330	FMW	7.32	6.95	8.05	6.99	6.66	6.93	—	—	—	—
Fe I	585.6087	-1.640	FMW	4.11	6.71	5.84	6.96	4.20	6.84	—	—	—	—
Fe I	585.8779	-2.260	FMW	2.26	6.84	3.55	7.05	1.95	6.86	—	—	—	—
Fe I	586.1109	-2.450	FMW	1.44	6.87	—	—	—	—	—	—	—	—
Fe I	587.7794	-2.230	FMW	—	—	—	—	3.24	7.09	—	—	—	—
Fe I	588.3817	-1.360	FMW	7.83	6.71	9.72	6.98	7.89	6.85	—	—	—	—
Fe I	595.2717	-1.440	FMW	—	—	9.04	6.95	—	—	8.37	6.70	9.59	6.98
Fe I	601.2210	-4.200	FMW	—	—	8.38	7.14	—	—	—	—	7.83	6.99
Fe I	601.5245	-4.680	FMW	—	—	—	—	—	—	—	—	3.44	6.76
Fe I	601.9366	-3.360	FMW	—	—	—	—	—	—	3.09	7.05	1.93	6.92
Fe I	602.4058	-0.120	FMW	—	—	11.97	6.95	—	—	11.65	6.82	11.97	6.86
Fe I	602.7051	-1.210	FMW	—	—	9.66	6.96	—	—	10.18	6.95	9.66	6.87
Fe I	605.6005	-0.460	FMW	—	—	7.92	6.74	—	—	8.29	6.76	9.24	6.92
Fe I	607.9008	-1.120	FMW	—	—	6.07	6.94	—	—	—	—	7.02	7.06
Fe I	609.6663	-1.930	FMW	—	—	6.65	6.96	—	—	7.28	6.97	6.79	6.94
Fe I	610.5128	-2.050	FMW	—	—	2.28	6.99	—	—	3.19	7.11	2.38	6.99
Fe I	612.0246	-5.950	FMW	—	—	—	—	—	—	—	—	6.37	6.67
Fe I	615.1616	-3.299	FMW	10.45	6.75	—	—	9.99	6.85	—	—	—	—
Fe I	615.9375	-1.970	FMW	—	—	—	—	—	—	—	—	2.93	7.11
Fe I	616.5360	-1.550	FMW	6.11	6.78	7.06	6.87	6.24	6.92	8.08	6.96	7.26	6.85
Fe I	618.7989	-1.720	FMW	6.77	6.81	8.20	6.98	—	—	8.64	6.95	7.72	6.83
Fe I	622.6734	-2.220	FMW	—	—	6.21	7.03	—	—	7.19	7.09	6.31	7.00
Fe I	649.6465	-0.570	FMW	7.25	6.836	6.99	6.73	7.39	6.97	—	—	7.49	6.76
Fe I	651.8366	-2.750	FMW	—	—	11.40	7.02	—	—	13.03	7.10	10.42	6.77
Fe I	659.7559	-1.070	FMW	—	—	5.86	7.02	—	—	6.54	7.10	5.99	7.00
Fe I	670.3565	-3.160	FMW	7.81	6.83	9.42	6.95	8.20	7.07	—	—	—	—
Fe I	672.5356	-2.300	FMW	—	—	4.39	7.06	—	—	5.29	7.11	—	—
Fe I	673.9521	-4.950	FMW	—	—	8.63	6.90	—	—	10.55	6.91	—	—
Fe I	674.6954	-4.350	FMW	—	—	3.42	6.92	—	—	4.84	6.94	3.52	6.92
Fe I	679.3258	-2.470	FMW	—	—	3.78	7.08	—	—	3.97	7.01	2.77	6.86
Fe I	684.2685	-1.320	FMW	—	—	6.36	7.14	—	—	6.71	7.14	6.12	7.05
Fe I	684.3655	-0.930	FMW	—	—	8.33	6.98	—	—	8.74	6.99	8.40	6.93
Fe I	685.7250	-2.150	FMW	—	—	—	—	—	—	—	—	4.10	6.79
Fe I	686.2492	-1.570	FMW	—	—	5.15	7.06	—	—	5.92	7.13	4.90	6.98
Fe I	691.6680	-1.450	FMW	—	—	8.68	7.02	—	—	10.25	7.20	8.96	7.00
Fe I	697.6922	-1.850	FMW	—	—	2.44	6.85	—	—	3.71	7.04	2.72	6.89
Fe I	698.8524	-3.660	FMW	—	—	—	—	—	—	12.04	7.12	10.40	7.02
Fe I	702.2952	-1.250	FMW	—	—	9.64	7.04	—	—	10.62	7.11	8.96	6.84
Fe I	706.9531	-4.340	FMW	—	—	4.00	6.93	—	—	5.03	6.87	—	—
Fe I	721.9682	-1.690	FMW	—	—	8.16	7.05	—	—	9.27	7.14	8.74	7.08
Fe I	747.6375	-1.680	FMW	—	—	2.71	7.00	—	—	—	—	3.73	7.17
Fe I	749.8530	-2.250	FMW	—	—	3.87	6.94	—	—	5.50	7.12	4.23	6.97
Fe I	758.3787	-1.990	FMW	—	—	14.44	6.90	—	—	15.74	6.90	15.71	7.00
Fe I	794.1087	-2.580	FMW	—	—	9.04	6.91	—	—	10.19	6.92	9.24	6.87
Fe I	883.8427	-1.980	FMW	—	—	17.12	6.92	—	—	—	—	18.18	6.97
Fe II	483.3197	-4.780	FMW	2.22	6.84	—	—	—	—	—	—	—	—
Fe II	499.3358	-3.650	FMW	—	—	6.27	7.12	4.65	6.88	—	—	—	—
Fe II	510.0664	-4.370	FMW	3.54	6.96	—	—	—	—	—	—	—	—
Fe II	513.2669	-4.180	FMW	—	—	3.50	7.01	3.01	7.01	—	—	—	—
Fe II	525.6937	-4.250	K88	3.08	6.82	2.90	7.03	—	—	—	—	—	—
Fe II	526.4812	-3.190	FMW	5.71	6.79	4.55	6.81	4.56	6.90	—	—	—	—
Fe II	599.1376	-3.557	K88	—	—	3.23	6.80	—	—	3.90	7.04	3.91	6.85
Fe II	608.4111	-3.808	K88	—	—	2.74	6.98	—	—	2.23	6.87	—	—
Fe II	614.9258	-2.724	K88	—	—	3.16	6.86	2.75	6.79	3.58	7.10	4.17	7.00
Fe II	624.7557	-2.329	K88	—	—	4.50	6.83	—	—	4.32	6.92	5.80	6.98
Fe II	636.9462	-4.253	K88	—	—	2.28	6.92	—	—	2.43	7.01	2.84	6.97
Fe II	643.2680	-3.500	H92	—	—	4.60	6.76	—	—	4.50	7.02	—	—
Fe II	645.6383	-2.075	K88	—	—	5.87	6.91	—	—	4.90	6.84	—	—
Fe II	651.6080	-3.380	H92	—	—	6.08	6.95	—	—	5.65	7.02	6.81	7.02
Co I	533.17**	-6.473	K88	HFS	4.19	HFS	4.28	HFS	4.32	—	—	—	—
Co I	553.07**	-2.060	FMW	HFS	4.02	HFS	4.35	HFS	4.27	—	—	—	—
Co I	609.34**	-4.568	K88	—	—	HFS	4.16	HFS	4.15	HFS	4.10	HFS	4.01
Ni I	493.5830	-0.350	FMW	—	—	7.40	5.49	—	—	—	—	7.33	5.40

Ni I	585.7746	-0.636	K88	4.37	5.43	5.36	5.61	4.47	5.60	—	—	—	—
Ni I	600.7306	-3.330	FMW	—	—	8.42	5.48	—	—	—	—	9.12	5.54
Ni I	608.6276	-0.530	FMW	—	—	4.01	5.37	—	—	4.67	5.45	4.83	5.48
Ni I	611.1065	-0.870	FMW	—	—	—	—	—	—	—	—	3.47	5.33
Ni I	612.8963	-3.330	FMW	—	—	9.04	5.58	6.28	5.44	—	—	—	—
Ni I	613.0130	-0.960	FMW	1.43	5.16	—	—	2.25	5.55	—	—	—	—
Ni I	617.5360	-0.530	FMW	5.01	5.33	5.32	5.39	5.35	5.55	5.34	5.33	5.93	5.44
Ni I	617.6807	-0.260	LW	6.42	5.33	7.04	5.44	6.77	5.56	—	—	—	—
Ni I	617.7236	-3.500	FMW	4.99	5.37	5.66	5.36	4.96	5.57	7.39	5.41	—	—
Ni I	618.6708	-0.960	FMW	—	—	—	—	—	—	—	—	3.30	5.41
Ni I	620.4600	-1.100	LW	—	—	2.46	5.38	—	—	2.84	5.39	2.83	5.43
Ni I	632.7592	-3.150	FMW	—	—	—	—	—	—	—	—	11.26	5.69
Ni I	648.2796	-2.630	FMW	—	—	10.77	5.51	—	—	12.10	5.51	10.99	5.46
Ni I	658.6307	-2.810	FMW	—	—	—	—	—	—	12.39	5.76	11.33	5.72
Ni I	659.8592	-0.980	FMW	—	—	—	—	—	—	—	—	2.88	5.50
Ni I	677.2313	-0.980	FMW	—	—	6.62	5.47	—	—	7.12	5.47	7.59	5.57
Ni I	700.1534	-3.660	FMW	—	—	—	—	—	—	—	—	5.49	5.55
Ni I	706.2951	-3.500	FMW	—	—	5.77	5.50	—	—	7.98	5.61	6.18	5.52
Ni I	778.8936	-2.420	FMW	—	—	—	—	—	—	—	—	14.92	5.71
Cu I	510.55**	-1.516	BIEL	HFS	3.14	HFS	2.91	HFS	3.22	—	—	—	—
Zn I	481.0528	-0.170	BG	6.20	3.39	7.83	3.88	6.94	3.81	—	—	—	—
Y II	488.3683	0.070	HL	—	—	—	—	9.58	1.64	—	—	—	—
Y II	498.2130	-1.290	HL	3.91	1.27	5.79	1.66	4.81	1.79	—	—	—	—
Y II	508.7417	-0.170	HL	7.63	1.02	8.56	1.18	8.51	1.57	—	—	—	—
Y II	511.9113	-1.360	HL	3.74	1.24	3.93	1.31	3.06	1.44	—	—	—	—
Y II	679.5413	-1.190	CC	—	—	1.72	1.54	—	—	3.48	1.79	1.67	1.47
Ba I	649.6897	-0.377	NBS	17.99	1.81	21.05	2.01	18.53	2.09	—	—	21.01	1.90
La II	480.4039	-1.500	LA	4.65	0.93	5.69	1.08	4.39	1.22	—	—	—	—
La II	511.4558	-1.030	LA	—	—	9.77	1.45	—	—	—	—	—	—
La II	632.0377	-1.610	ABH	4.89	0.87	7.14	1.21	3.71	1.00	9.46	1.27	6.21	0.98
La II	639.0477	-1.410	LA	4.33	0.75	5.07	0.86	3.78	1.00	7.31	0.90	4.95	0.78
Ce II	518.7457	0.130	H	4.19	1.14	5.53	1.41	4.84	1.62	—	—	—	—
Ce II	533.0556	-0.360	H	2.98	0.92	4.00	1.13	3.59	1.40	—	—	—	—
Nd II	491.4382	-0.700	HA	6.39	1.15	8.90	1.61	6.15	1.44	—	—	—	—
Nd II	496.1387	-0.710	MC'	5.26	1.22	7.25	1.58	5.83	1.69	—	—	—	—
Nd II	498.9950	-0.500	MC'	—	—	10.13	2.03	7.26	1.82	—	—	—	—
Nd II	499.8540	-1.100	MC'	3.36	1.00	4.96	1.28	3.20	1.31	—	—	—	—
Nd II	508.9832	-1.160	MC'	4.42	0.93	5.96	1.15	4.77	1.35	—	—	—	—
Nd II	543.1515	-0.470	HA	2.87	1.05	3.54	1.22	2.19	1.23	—	—	—	—
Nd II	548.5097	-1.640	HA	—	—	3.28	1.57	—	—	—	—	—	—